

AD-A118 677

ARMY ARMAMENT RESEARCH AND DEVELOPMENT COMMAND DOVER--ETC F/G 19/1
THE CORRELATION OF NITROCELLULOSE PROPERTIES AND CELLULOSE FEED--ETC(U)
JUL 82 H J PRASK, C S CHOI
ARLCD-TR-82011

SBI-AD-E400 878

NL

UNCLASSIFIED

Incl

1

2

3

4

5

6

7

8

9

10

11

12

13

14

15

16

17

18

19

20

21

22

23

24

25

26

27

28

29

30

31

32

33

34

35

36

37

38

39

40

41

42

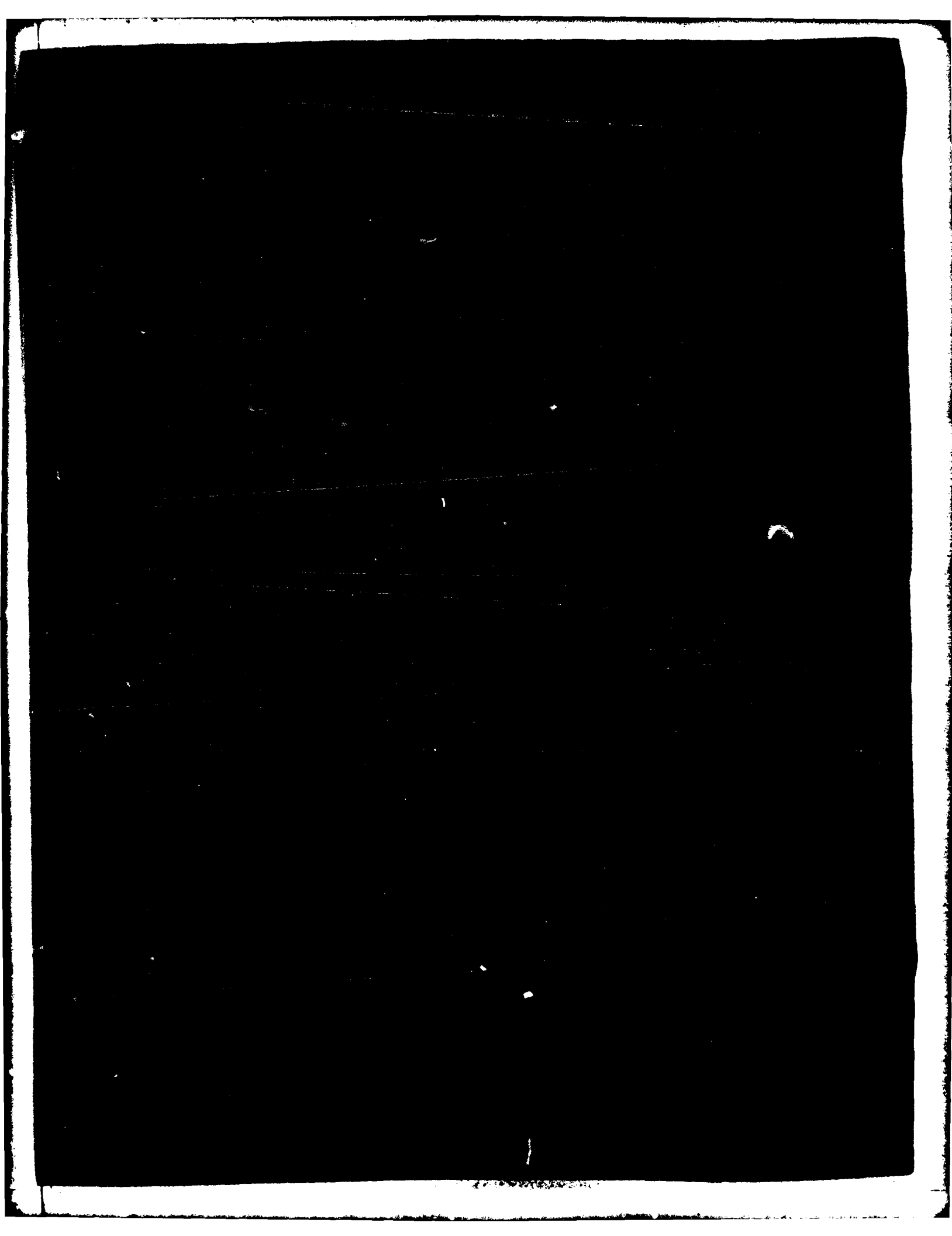
43

44

45

END
DATE
FILMED
9 82
DTIC

AD A118677



UNCLASSIFIED

SECURITY CLASSIFICATION OF THIS PAGE (When Data Entered)

REPORT DOCUMENTATION PAGE		READ INSTRUCTIONS BEFORE COMPLETING FORM
1. REPORT NUMBER Technical Report ARLCD-TR-82011	2. GOVT ACCESSION NO. AD-A18677	3. RECIPIENT'S CATALOG NUMBER
4. TITLE (and Subtitle) THE CORRELATION OF NITROCELLULOSE PROPERTIES AND CELLULOSE FEEDSTOCK CRYSTAL STRUCTURE		5. TYPE OF REPORT & PERIOD COVERED FINAL 1980-1982
		6. PERFORMING ORG. REPORT NUMBER
7. AUTHOR(s) H. J. Prask and C. S. Choi		8. CONTRACT OR GRANT NUMBER(s)
9. PERFORMING ORGANIZATION NAME AND ADDRESS ARRADCOM, LCWSL Energetic Materials Div (DRDAR-LCE) Dover, NJ 07801		10. PROGRAM ELEMENT, PROJECT, TASK AREA & WORK UNIT NUMBERS
11. CONTROLLING OFFICE NAME AND ADDRESS ARRADCOM, TSD STINFO Div (DRDAR-TSS) Dover, NJ 07801		12. REPORT DATE July 1982
14. MONITORING AGENCY NAME & ADDRESS (if different from Controlling Office)		13. NUMBER OF PAGES 51
		15. SECURITY CLASS. (of this report) UNCLASSIFIED
16. DISTRIBUTION STATEMENT (of this Report) Approved for public release; distribution unlimited.		15a. DECLASSIFICATION/DOWNGRADING SCHEDULE
17. DISTRIBUTION STATEMENT (of the abstract entered in Block 20, if different from Report)		
18. SUPPLEMENTARY NOTES		
19. KEY WORDS (Continue on reverse side if necessary and identify by block number) Cellulose Total-profile analysis Woodpulp Cotton linters X-ray diffraction Nitrocellulose		
20. ABSTRACT (Continue on reverse side if necessary and identify by block number) Studies of cellulose crystallinity are reviewed. The total-profile analysis method has been applied to x-ray diffraction data for celluloses from linter and woodpulp sources. Good agreement is obtained with published structure factors and lattice parameters from fiber studies, if a distinct amorphous profile is included in our analysis. Correlations between cellulose and nitrocellulose properties and the measured cellulose crystallographic parameters are indicated.		

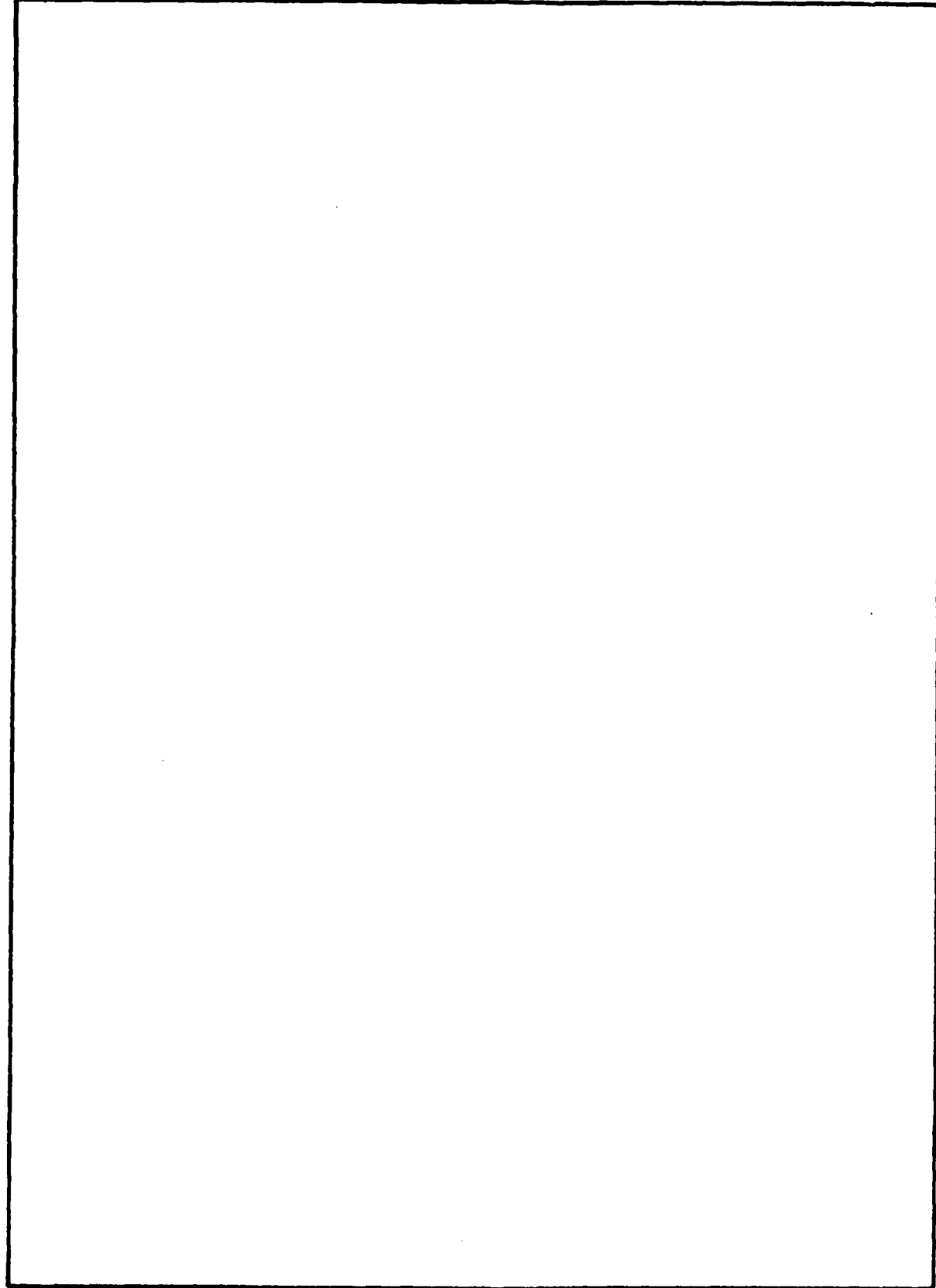
DD FORM 1 JAN 73 1473

EDITION OF 1 NOV 65 IS OBSOLETE

UNCLASSIFIED

SECURITY CLASSIFICATION OF THIS PAGE (When Data Entered)

SECURITY CLASSIFICATION OF THIS PAGE(When Data Entered)



SECURITY CLASSIFICATION OF THIS PAGE(When Data Entered)

CONTENTS

	Page
Introduction	1
Background	1
Cellulose Crystal Structure	1
Crystallinity	2
X-ray Total Profile Analysis	3
Crystallinity and Macroscopic Properties	3
Method	4
Experimental	4
Analysis Formalism	4
Analysis Details	6
Results	8
Cellulose: Lattice Parameters and Relative Intensities	8
Cellulose: Crystallinity, Phase Concentrations, and Crystallite Size	10
Nitrocellulose: Crystallographic Studies	11
Nitrocellulose: Other Characterization	12
Discussion	13
Cellulose	13
Cellulose/Nitrocellulose Correlations	14
Conclusions	15
Recommendations	16
References	17
Distribution List	43



Accession For	
NTIS GRA&I	<input checked="" type="checkbox"/>
DTIC TAB	<input type="checkbox"/>
Unannounced	<input type="checkbox"/>
Justification	
By _____	
Distribution/	
Availability Codes	
Dist	Avail and/or Special
A	

TABLES

	Page
1 Cellulose samples	21
2 Secondary Bragg reflections	22
3 Linters: lattice parameters and peak intensities	23
4 Fortisan: lattice parameters and peak intensities	24
5 Woodpulp: lattice parameters and peak intensities	25
6 Celluloses: crystallinity, particle sizes, and shape parameters	27
7 Total-profile refinement parameters for 13.5 wt% N, linter NC	28
8 d-spacing and FWHM of NC(101) reflection	29
9 Various other properties of celluloses	30

FIGURES

		Page
1	Crystallographic phases and possible interconversions of cellulose and tri-nitrocellulose polymorphs	31
2	X-ray diffraction patterns for cellulose	32
3	X-ray diffraction pattern of Hercules NS-70 (sheet) linters with total-profile fits and (amorphous + Compton + secondary Bragg peaks) contribution	33
4	X-ray diffraction pattern of cellulose II with various calculated contributions	34
5	X-ray diffraction patterns of various woodpulp celluloses with total-profile fits and (amorphous + Compton + secondary Bragg peaks + cellulose I) contributions	35
6	X-ray diffraction pattern of Buckeye N-5 with various calculated contributions	36
7	Schematic representation of unit cells comprising a cellulose I crystallite, viewed along the chain axis with crystallite dimensions for various directions indicated ($2\ell = L$ of table 6)	37
8	X-ray diffraction patterns of selected NC samples	38
9	X-ray diffraction pattern of Hercules-linter guncotton with total-profile fit and amorphous contribution using parameters on table 7	39
10	$d(101)$ versus percent nitrogen	40
11	NC viscosity versus cellulose viscosity for pyrocottons (closed circles) and guncottons (open circles)	41
12	Crystallite (002) dimension versus percent-solubility and Mullen Burst Strength for woodpulp	42

INTRODUCTION

The two major sources of cellulose for nitrocellulose (NC) production are cotton linters and woodpulp. In general, although not without exception, cotton linters provide a uniform source for NC, suitable for both batch and continuous nitration production methods. However, linters are more expensive than pulps and could be in short supply if present production facilities were fully mobilized. In contrast, woodpulp offers a considerably less uniform, but plentiful and less costly source of cellulose for NC.

In order to provide NC manufacturing facilities with reasonably uniform woodpulp feedstock, a program begun in the early 1950s established process control parameters for pulps for use in NC manufacture by the batch process (ref 1). Despite the controls, occasional batches of acceptable NC were produced which were difficult to process into propellant. In batch-process production gradual blending was possible to utilize all NC. However, the development of continuous nitration and propellant processing lines limits flexibility in production and dictates more stringent controls on pulp variables to prevent formation of difficult-to-process propellant.

Several recent ARRADCOM-sponsored studies have focused on the development of improved process control and acceptance requirements for woodpulp for continuous-line propellant production (refs 2 through 4). Of these, Bracuti (ref 2) and Prask et al. (ref 3) employed already-developed techniques for analysis of x-ray diffraction data to determine critical microscopic structural parameters for cellulose feedstock from different sources. Mundy et al. (ref 4) used conventional analytical chemical techniques to characterize and contrast celluloses and the NC prepared therefrom.

In the present work we significantly extend the x-ray diffraction approach for characterization of microscopic structural properties of cellulose. In addition we relate structural properties of a variety of celluloses and properties of NC prepared therefrom. Although emphasis is placed primarily on the elucidation of the microscopic structure of different celluloses, there is abundant evidence indicating a correlation between microscopic structure and macroscopic properties such as strength and embrittlement. More importantly, analogous behavior would be expected for NC, an area which has not yet been investigated.

BACKGROUND

Cellulose Crystal Structure

Crystallographically, cellulose is a very complex material and because of its technological importance has been the subject of a large number of crystallographic studies spanning several decades (ref 5). The current view is that crystalline cellulose occurs in at least four distinct structures, the interrelationships of which are indicated in figure 1 (ref 6). The four principal forms are distinguishable by diffraction methods; however, in the context of NC production, forms I and II are of principal interest and only these will be considered explicitly.

Although there is some controversy concerning the detailed structure of cellulose I from certain sources, for practical purposes both cellulose I and II are monoclinic in structure. Wellard (ref 7) has determined lattice parameters for forms I and II from a number of different sources and finds a large range of values. However, for cellulose I from Ramie and cotton, he found $a \approx 8.17$, $b \approx 10.34$, $c \approx 7.855$ A, and $\beta \approx 83.5^\circ$. In the case of cellulose II, mercerized Ramie yields $a = 7.97$, $b = 10.34$, $c = 9.22$ A, and $\beta = 62.2^\circ$, while Fortisan gives $a = 7.92$, $b = 10.34$, $c = 9.08$ A, and $\beta = 62.7^\circ$. More recently, Kolpak et al. (ref 8) have studied mercerized cotton (II) and obtained $a = 8.02$, $b = 10.36$, $c = 8.99$ A, and $\beta = 63.4^\circ$ while Woodcock and Sarko (ref 9) obtained, for native Ramie cellulose I, $a = 8.20$, $b = 10.34$, $c = 7.78$ A and $\beta = 83.5^\circ$. Overall, the structure of cellulose II is less open than that of cellulose I which has significance with respect to solvent penetration in the nitration process.

Crystallinity

The term "crystallinity" applied to polymers refers to the fact that in a single sample the long chain molecules can be found in states ranging from a highly-ordered array (crystalline) to a completely disordered array (amorphous). Because of the importance of the degree of crystallinity in determining mechanical properties (discussed in a later subsection) attempts to measure crystallinity have paralleled studies of crystal structure *per se*. The exact nature of noncrystallinity in cellulose has been pictured as ranging from a model in which two phases, crystalline and amorphous occur, each distinct and homogeneous, to the more plausible model of Hovsmo (ref 10) which includes varying degrees of order, to the structure of Hosemann (ref 11), in which no highly disordered regions occur, but rather various distortions of a crystalline structure.

Many different experimental techniques have been used to measure crystallinity of cellulose, and the results are rarely in agreement. Mann (ref 12) has stated that the techniques most closely related to the presence of intermolecular order in a substance are its diffraction pattern and its infrared spectrum. Of these, diffraction must be the basic tool for crystallization studies because of the direct relation between diffraction and order. Indeed, x-ray diffraction has been the primary technique for crystallinity studies, but even with x-rays, different approaches have yielded vastly different estimates of crystallinity.

Methods of extracting crystallinity of cellulose from x-ray diffraction measurements have been reviewed (refs 13 and 14). Types of approaches range from the highly empirical types which infer crystallinity from the width of the (002) reflection, or the ratio of (002) peak height to "amorphous intensity" at 18.2° (fig. 2), to the elegant analysis of Ruland (ref 15), applied to celluloses in ref 16, in which crystalline fraction, amorphous fraction, and imperfection parameter are inferred without using external standards and without analyzing individual peak shapes. In contrast to Ruland's approach, there has been a body of investigations which aim not only at the determination of crystallinity, but also attempt to characterize such properties as crystallite size and elastic strains from detailed analysis of the total diffraction profile including peak shapes and widths. In general, both Ruland's approach and the total-profile approach require a choice of separation of crystalline and noncrystalline contributions to the diffraction pattern.

X-ray Total Profile Analysis

One of the first attempts to analyze the total profile of the principal diffraction peaks of cellulose I and II was reported by Gjonnes et al. (ref 17) in 1958. Assuming that the crystalline-fraction peaks were Cauchy in shape, they concluded that virtually no amorphous component was necessary to explain the cellulose I pattern. In the case of cellulose II, they found excess scattering which could be accounted for by an amorphous component. They concluded that cellulose I and II were 95 and 60 percent crystalline, respectively. Later Hermans and Weidinger (ref 18) analyzed the principal reflections from cellulose I fibers. No specific conclusions were drawn concerning degree of crystallinity or particle sizes.

More recently, Hindeleh and Johnson (ref 19) have performed a total-profile analysis of equatorial diffraction peaks for fibers of Ramie and Fortisan. Details of their approach will be provided in the next section. They extract both crystallinity and crystallite sizes and include a noncrystalline component of arbitrary shape. Krassig (ref 20) reported results of studies of several cellulose samples including mixtures of forms I and II. Following Gjonnes et al. (ref 17), he concluded that not only are Cauchy peak shapes appropriate, but that no explicit amorphous profile was required to explain the diffraction patterns. He proposed that the amorphous component required by Gjonnes et al. to best explain their cellulose II results was actually residual cellulose I not completely converted in the mercerization process.

Crystallinity and Macroscopic Properties

Bracuti (ref 2) has described some of the possible chemical effects of degree of crystallinity on the nitration of cellulose. In this subsection we describe some results which relate mechanical properties and crystallinity. Atalla (ref 21) has recently reported on the relationship of crystallinity in cellulose and properties of importance in the textile and paper industries. We believe that results of this nature are equally relevant to the aging and embrittlement of NC-containing propellants, an area which has not yet been explored.

Atalla proposes that the greater the order in a polymeric structure, the less able the structure is to absorb mechanical energy elastically. He found that such properties as tensile strength and burst and tear properties of paper all decreased with exposure of samples to temperatures of the kraft cycle (i.e., accelerated aging), and that the deterioration correlated with changes in "crystallinity." It should be mentioned, however, that Atalla's measure of crystallinity was the width of the (002) reflection which, as we will discuss, is more properly associated with particle size and/or residual strains rather than the crystalline-fraction concentration usually called "crystallinity."

In contrast to aging effects considered by Atalla, Mannan and Reazuddin (ref 22) have studied the breaking strength of fibers and have shown a very clear correlation with crystallinity (as determined by Ruland's method). They find that breaking strength is directly proportional to crystallinity for seven samples with crystallinities in the range 43 to 65% (extrapolating to ~ 0 strength at 0% crystallinity).

METHOD

Experimental

X-ray diffraction measurements were made with a computer-controlled Norelco diffractometer in the symmetric reflection configuration with $1/2^\circ$ divergence for incident and diffracted beams. $\text{CuK}\alpha$ radiation filtered with nickel foil was used. Diffraction data were collected in 0.2° steps over the range 4 to 80° in 2θ and stored directly in a DEC 1140 computer. All measurements were made at the National Bureau of Standards, Reactor Radiation Division.

Cellulose samples were prepared by mechanically shredding the material and then pressing 250 mg quantities into 1.3 cm diameter pellets at 2000 kg/cm^2 for 2 minutes. NC samples prepared from the various celluloses (details of nitration in ref 4) were removed from water storage, manually pressed into a 2 cm diameter by 0.2 cm deep sample holder cavity and air dried. Both types of samples were rotated continuously about their cylindrical axes during measurements.

The amorphous standard was prepared from a cotton linter sample. Vibratory ball-milling for 2 hours was followed by pelletizing as described above.

In table 1 are listed the different cellulose samples studied.

Analysis Formalism

The determination of crystallinity by means of the total-profile method, reviewed briefly in a previous subsection, is particularly attractive because of the amount of information that can, in principal, be obtained (i.e., crystallinity, lattice parameters, crystallite sizes, elastic strains). Two of the most recent studies employing this technique, Krassig's (ref 20) and Hindeleh and Johnson's (ref 19), differ fundamentally in their conclusions. However, in neither case do they constrain their least-squares analyses of the principal reflections to a monoclinic structure, nor do they compare their measured relative intensities with known structure factors. Furthermore, Krassig (as well as Gjonnes et al. (ref 17)) who studied unoriented powders, takes no account of the numerous, relatively weak non-equatorial reflections which contribute to diffracted intensity.

The present work differs significantly from earlier work in the following ways: 1) We constrain the structures for all samples to be monoclinic but refine lattice parameters and compare with expected values; 2) In addition to the principal reflections, we include other expected reflections, scaled to account for orientation effects; 3) We extract relative peak intensities and compare with structure factors obtained from careful crystal structure measurements on fibers; 4) We make use of an explicit noncrystalline profile (ball-milled cellulose) which Mann (ref 12) has shown is very similar to a weak halo observed in the regions between strong reflections in studies of highly-oriented fiber samples. Mann also proposed that the use of the profile of ball-milled cellulose as a standard for amorphous cellulose is valid regardless of the exact character of the noncrystalline regions (see "Crystallinity"

subsection); 5) Following Hindeleh and Johnson, a Bragg peak profile of mixed Gaussian and Cauchy character is included; and 6) The analysis incorporates a provision for mixed cellulose I and cellulose II samples.

The total diffraction profile for the cellulose samples can be represented formally as

$$I(\theta) = B(\theta) + A(\theta) + \sum_{i,k} Q^{ik}(\theta) \quad (1)$$

where θ is the scattering angle ($\theta/2$ is the Bragg angle), $B(\theta)$ is a background comprised of air scattering, electronic noise, etc., $A(\theta)$ is the amorphous/non-crystalline contribution, and following reference 19, the crystalline reflections are given by

$$Q^{ik}(\theta) = f^i H^{ik}(\theta) \exp \left\{ -\ln 2 \left[\frac{2(\theta - \theta_o^{ik})}{W^{ik}} \right]^2 \right\} + \frac{(1-f^i) H^{ik}(\theta)}{1 + 2(\theta - \theta_o^{ik})/W^{ik}} \quad (2)$$

where the i,k subscripts denote the k th reflection (e.g. 002) of the i th form (e.g. cellulose I). This differs from references 19 and 20 in that we do not refine the peak positions θ_o^{ik} directly but instead

$$\theta_o^{ik} = \theta_o^{ik} (A_i, B_i, C_i, \beta_i, h_{ik}, k_{ik}, l_{ik}) \quad (3)$$

where A_i, B_i, C_i, β_i are the monoclinic lattice parameters of form i , which are refined, and h_{ik}, k_{ik}, l_{ik} are the Miller indices of the included reflections. In equation 2, f^i is the Gaussian fraction of form i (i.e., $f = 1 =$ all Gaussian; $f = 0 =$ all Cauchy); H^{ik} is the amplitude of the i,k th peak and W^{ik} is the full width at half maximum height (FWHM) of the i,k th peak.

The peak shape defined in equation 2 was proposed by Hindeleh and Johnson to incorporate broadening effects due to particle size (Cauchy) and elastic strains (Gaussian). A more rigorous approach would convolute the particle size and strain effects; that is, the measured profile is actually a Cauchy profile, broadened point-by-point by a Gaussian profile, finally broadened by instrumental resolution. The deconvolution of such profiles, particularly for the overlapping diffraction peaks of cellulose, is not feasible. Similarly, the f -parameter of equation 2 is assumed to be identical for all planes in the i th form. A more rigorous treatment would allow different crystallite dimensions and strains in different directions i.e., for different reflections. Again, for the overlapping peaks of the cellulose patterns, incorporating this feature is of questionable value.

Analysis Details

X-ray Correction Factors

The procedure used in the least-squares analysis was to multiply the calculated peaks by appropriate correction factors and refine against experimental data. The corrections included Lorenz and polarization factors, absorption, a sample size factor, and Compton scattering. Air scattering was judged to be negligible above $\theta \gtrsim 8^\circ$. Absorption corrections were calculated from the atomic absorption coefficients (ref 23) and measured thickness and density of each sample. The sample size correction accounts for the fact that at small scattering angles ($\theta \lesssim 15^\circ$), not all of the x-ray beam strikes the sample so that a distorted $I(\theta)$ is measured. Following Ruland (ref 15), a Compton profile as a function of θ is obtained from theoretical calculations of the incoherent scattering functions: carbon (ref 24), hydrogen (ref 25), and oxygen (ref 26).

Orientation Effects

In pressed pellet samples of polymers, unless extreme care is taken to cut the fibers into very small lengths, pronounced preferred orientation will occur. Comparison of figures 2a and 2b show preferred orientation clearly, particularly at the (021) reflection and for $\theta \gtrsim 27^\circ$. Segal et al. (ref 27) have cited this as an advantage in that amorphous-component peak intensity (at $\theta \sim 18^\circ$) is easier to determine. Our and other work shows that the crystalline peaks contribute intensity at $\theta \sim 18^\circ$ even with preferred orientation (cf. figs. 3 and 5). More recently, Ivanov and Kosoy (ref 28) have noted that the amorphous component, by definition, is unoriented even in a sample the crystalline component of which is textured. They propose a somewhat oversimplified scheme to deduce a crystallinity index by comparing completely amorphous cellulose with other samples at $\theta = 32^\circ$ where crystalline reflection contributions are minimal. In our approach we assume only that whatever preferred orientation is present in the amorphous standard is also present in the amorphous component of the test sample.

Normalization

Proper normalization is required for the several different components of each pattern to achieve a correct quantitative deconvolution. Assuming that the samples are identical in chemical composition, the calculated scattering patterns are multiplied by sample density to account for density variations. Sample-to-sample instrumental variations are corrected for by rescaling all patterns to give the amorphous standard intensity in the $74^\circ \lesssim \theta \lesssim 78^\circ$ region, after correction for polarization, absorption, and density differences. The Compton contribution to each pattern is assumed identical (after the rescaling described above). The relative intensity is determined from the ratio of calculated coherent to incoherent structure factors at $\theta = 31^\circ$ and scaled according to the total intensity measured for the amorphous standard at this angle (ref 14).

Adjustable Parameters

Equations 1 and 2 show, formally, the various components of the total profile of the cellulose diffraction patterns. However, because of the intrinsic breadth, and resultant overlap, of the cellulose diffraction peaks, not all components can be freely refined. In our approach, as many parameters as possible are constrained in order to achieve physically meaningful results:

a) The amorphous profile (fig. 2d) is least-squares fit by a sum of six Gaussian peaks of arbitrary amplitude, width, and peak position;¹ the amorphous component for any test sample is then a single (refined) amplitude parameter times the analytical amorphous profile.

b) The lattice parameters for only the principal form of cellulose present are refined. For the test samples studied, it turned out that any admixed form was present in such low concentration that its principal peaks were obscured and lattice parameters could not be refined. Consequently, a procedure analogous to that for the amorphous fraction was employed; that is, an amplitude parameter multiplied a diffraction profile for the admixed component.

c) The fiber-axis lattice parameter (b-axis) was not refined because orientation effects diminished nonequatorial reflection intensities. The results of reference 8 (cellulose II) and reference 9 (cellulose I) were used for b values.

d) Nonequatorial reflections were included but not refined explicitly. The more intense reflections were selected from the observed reflections of references 8 and 9, and their contribution to the diffraction patterns scaled to either the refined (021) or (002) reflections. However, as appropriate, nonequatorial reflections were scaled by an "orientation" factor, discussed in more detail in the Results section.

e) A flat background was assumed.

The analytic expression for the total diffraction profile then takes the form:

$$\begin{aligned} I(\theta) = & P_{BG} + \text{COMP}(\theta) + P_{AM} \cdot \text{AMORPH}(\theta) \\ & + P^j \cdot \text{CELL}(j, \theta, WM) + SC \cdot \text{CELL}(1, \theta) \\ & + \sum_k Q^{ik}(\theta) \end{aligned} \quad (4)$$

¹ The relative amplitudes, positions, and FWHMs of the six Gaussian peaks which comprise the amorphous profile from $8^\circ < \theta < 50^\circ$ are -0.58 , 17.46° , and 3.63° ; 4.13 , 20.35° , and 9.17° ; 2.33 , 22.93° , and 3.37° ; -1.54 , 24.21° , and 2.16° ; -0.46 , 32.54° , and 2.43° ; and 6.74 , 46.04° , and 34.48° .

where

$$Q^{ik}(\theta) = \sum_k P_H^{ik}(\theta) \left\{ P_f^i \exp \left\{ -\ln 2 \left[\frac{2(\theta - \theta_o^{ik})}{P_W^{ik}} \right]^2 \right\} \right. \\ \left. + \frac{(1 - P_f^i)}{1 + [2(\theta - \theta_o^{ik})/P_W^{ik}]^2} \right\} \quad (5)$$

In equation 4 the terms on the right correspond, respectively, to a flat background, Compton scattering, the amorphous contribution, the diffraction profile of the lower concentration cellulose phase (j), the contribution of the weaker reflections of the principal phase (i), and the principal reflections of the principal phase. The various P_s are amplitude parameters adjusted in the refinement; WM is a FWHM multiplier, and SC is the orientation-dependent scaling factor determined empirically but not adjusted. In equation 5, P_H , P_f , and P_W are respectively the height, Gaussian fraction, and FWHM of the principal reflections of the principal phase. The θ -dependence of P_H denotes that the various angle-dependent corrections are included. The peak positions θ_o^{ik} are determined from

$$\theta_o^{ik} = \theta_o^{ik} (P_A, B, P_C, P_\beta, h^k, l^k, k^k) \quad (6)$$

for the monoclinic structure, where P_A , P_C , and P_β are the adjusted lattice parameters and the h , k , l are Miller indices.

RESULTS

Cellulose: Lattice Parameters and Relative Intensities

Cotton Linter Samples - Cellulose I

The three cotton linter samples studied showed the clearest resolution of peaks and as expected, no evidence of cellulose II. The nonequatorial reflections were scaled to the (021) reflection in the refinement. That is, the reflections listed in table 2 were included in the refinement with intensities fixed as dictated by the structure factors of reference 9, relative to the refined (021) intensity. In this procedure we neglect, as a first approximation, the fact that different reflections of the set may have different widths and different orientation effects.

In table 3 lattice parameters and integrated intensities for the principal reflections are listed and compared with fiber measurements. The refined lattice parameters and intensities are in reasonably good agreement with the range of values of the fiber measurements. If the same sort of comparison is made for other total-profile measurements (refs 17, 19, and 20), lattice parameters are in poorer agreement,² and integrated intensities, normalized to (002), are factors of 2 or 3 different than the fiber values.

² We determined lattice parameters from their measured peak positions and the known wavelengths.

In figure 3, three least-squares fit results to the sample 3 data are shown. Figure 3a shows the results if the Cauchy-Gaussian line-shape parameter and the amorphous-standard amplitude are adjusted (along with lattice parameters, peak widths and amplitudes, and background). In figure 3b, results are shown with the same parameters adjusted, but allowing only Cauchy peak profiles. In figure 3c, peak profiles are Cauchy and the amorphous-standard contribution is fixed at zero (as in refs 17 and 20). In each case, the nonequatorial reflections are included, scaled to the (021) intensity. It is clear that when the monoclinic structure constraint and fixed amorphous profile are required, the best results are obtained with a nonzero amorphous component and a mixed Cauchy-Gaussian peak profile.

Fortisan-Cellulose II

The refinement procedure for cellulose II is more complex than that for the cotton linter samples and requires all of the components included in equation 4. Following Krassig (ref 20), a residual cellulose I component is assumed possible. For simplicity, a cellulose I fraction with the average characteristics of the three linter samples is assumed (i.e., lattice parameters and relative peak intensities). A provision for expanding or contracting all peak widths proportionally is also included. In the case of the unresolved reflections (listed in table 2), all reflections are scaled to the refined (002) intensity according to the cellulose II structure factors of reference 8. In addition, nonequatorial reflections are reduced by an orientation scaling factor, the value of which is obtained from the cotton linter values:

$$SC = \frac{\bar{I}(021)_{\text{meas.}}}{I(002)_{\text{meas.}}} \cdot \frac{I(021)_{\text{ref. 9}}}{I(002)_{\text{ref. 9}}} \quad (7)$$

In the refinement, the cellulose I peak-width scaling factor was not freely adjusted. The procedure was to set this parameter, calculate the cellulose I profile, then refine the cellulose I overall amplitude parameter (p^j of equation 4) in the full least-squares fitting. It should be mentioned that for all samples, the unresolved Bragg peak profile is adjusted in the same way with regard to lattice parameters, FWHM, and Cauchy-Gaussian parameter.

For the samples studied, it turned out that the goodness-of-fit is not very sensitive to the widths of the cellulose I peaks. However, the relative intensities of the principal cellulose II Bragg peaks are. Therefore, the cellulose I width scaling factor was adjusted until good agreement with the fiber measurement structure factors was achieved ($WM = 2.1$). The data and the various component profiles are shown in figure 4. In table 4 is a partial list of the refined parameters.

Our refined values for the lattice parameters of cellulose II are not in as good agreement with the most complete fiber studies as the results for the cotton linter samples. However, the values do fall in the range of Wellard's values (ref 7). Lattice parameters obtained from other total-profile studies of cellulose II are reasonably good (ref 17) or fair (ref 20) compared to Wellard's range (table 4). The data of Hindeleh and Johnson (ref 19) for Fortisan appears to require a zero correction. However, as in the cellulose I case, the relative integrated intensities appear factors of 2 or 3 different than those expected from the measured structure factors from fiber studies.

Woodpulp

A total of eight woodpulp samples were analyzed with the diffraction technique described: two sulfite-process pulps and six sulfate-process pulps. Representative diffraction patterns and least-squares fit profiles are shown in figure 5. In each case a possible cellulose II component was included in the refinement. However, only sample 10 (fig. 5d) contained a significant amount (i.e., $P^j > \sigma$ (P^j)) of cellulose II, with $WM = 0.67$. The lattice parameter and relative intensity results are summarized in table 5. It should be noted that because of the breadth of the diffraction peaks in these samples, integrated intensities of the (101) and (10 $\bar{1}$) reflections are highly coupled. Therefore, a comparison is also made of relative intensities of [(101) + (10 $\bar{1}$)] with fiber values.

It is interesting that the refined (021) intensities for most of the woodpulp samples are in reasonable agreement with the linter values even though the (021) peaks are virtually invisible in the raw data. Also, except for samples 5, 11, and 12 the (101) + (10 $\bar{1}$) relative intensities are in excellent agreement with the linter values. It should be noted, however, that refinement of model parameters for samples 6 and 11 presented some problems. In the case of sample 6, no special constraints were required; nevertheless, some additional scattering intensity occurred in the 18° to 21° region which was not well fit with the model (fig. 5c). In the sample 11 case, the peaks were so broad that a constraint of 0.6 was imposed on the Cauchy/Gaussian fraction parameter before refinement was possible. Because of the peak widths the percent-crystallinity of sample 11 (table 6) is not believed to be very reliable.

Cellulose: Crystallinity, Phase Concentrations, and Crystallite Size

The results described in the previous subsection show that the proposed method yields lattice parameters and relative peak intensities which are consistent with recent fiber measurements. In this subsection we report additional results of the refinements which are indicative of the differences among the several samples studied.

Crystallinity is extracted directly from the least-squares refined parameters after all sample data are normalized to the high-angle intensity of the amorphous standard and the various corrections, discussed previously, are performed. This procedure scaled all measurements to scattering per unit sample weight. The amplitude of the amorphous fraction is refined directly and the crystallinity is simply: $1 - f_{AMORPHOUS}$. Values for the various samples are shown in table 6.

To determine the weight fraction of the minor component in a mixed sample, the amplitude (P^j) is obtained from the least-squares refinement. The intensity is directly proportional to P^j and the width (WM). The approximate weight fraction is then the intensity of the minor component in the mixed sample relative to the intensity/(crystalline sample weight) for the reference sample. More specifically, from the measured $I(002)$ intensity and the determined crystallinity for the renormalized data, an $I(002)/(100\% \text{ crystalline sample})$ is obtained for each single-phase sample. $I(002)$ of the minor component in the mixed sample is compared with this to get the minor component concentration.

In an ideally polycrystalline sample $I(002)/(100\%$ crystalline sample) would be identical or decrease with "degree of distortion." In our case we find that of the cellulose I samples, linters have smaller values than the pulps. We attribute this to differences in texture for the types of samples. To obtain an approximate concentration of cellulose I in Fortisan, we use the average of $I(002)_{100\%}$ for samples 1 through 3 and 5 through 9. For the weight fraction of cellulose II in sample 10, we use $I(002)_{100\%}$ of Fortisan. The obtained values are listed and shown graphically in figures 4 and 6.

As discussed earlier, the peak-shape parameter as employed by Hindeleh and Johnson (ref 19) and in this work is an approximation in several respects. The values obtained in the refinements are listed in table 6 and range from 50 to 85% Cauchy. Attributing these variations, quantitatively, to crystallite size or strain effects is a questionable procedure; nevertheless, we follow Hindeleh and Johnson and extract crystallite size parameters by means of the Debye-Scherrer equation and measured FWHMs, corrected for resolution broadening.

If we assume that a crystallite of cellulose I has the shape shown in figure 7, then from the measured (101) , $(10\bar{1})$, and (002) reflection widths, approximate dimensions along $[001]$ and $[100]$ can be extracted. This procedure averages the (101) and $(10\bar{1})$ widths, and to some extent, compensates for the coupling of the widths of these two modes in the refinement. The refined FWHMs and crystallite dimensions are shown in table 6.

Nitrocellulose: Crystallographic Studies

NC has been the subject of extensive x-ray diffraction study, beginning in the 1920s. Results to about 1960 have been reviewed and summarized in reference 31; more recent studies of NC have been reported by Watanabe and co-workers (refs 32 through 36). Despite the large body of results reported in the scientific literature, detailed knowledge of the crystallography of NC is extremely limited compared to cellulose. For example, although two forms of highly nitrated NC have been reported, no structural details other than structural type (i.e., orthorhombic) and lattice parameters are known (refs 31, 32, and 33). In addition, no analysis of NC in terms of amorphous and crystalline structures has ever been presented. The principal reason cited for the difficulty in analyzing NC diffraction data is the generally diffuse character of the diffraction pattern, even for fibers. Watanabe and co-workers have shown that features of the diffraction pattern can be sharpened considerably by treating NC with superheated water. Using this treatment they were able to obtain some important new information; however, details of structure and crystallinity were still not obtained.

In our first effort we do not make use of the treatment suggested by Watanabe. Furthermore, the samples examined were not optimized in shape or density. Nevertheless, some information of interest is obtained from the diffraction patterns. Analogous to the results for cellulose, we find qualitative differences in the diffraction patterns of guncotton from linters and woodpulp. Also, as is expected from other work, we see some differences as a function of nitration. Representative data illustrating these differences are shown in figure 8.

In figure 9, we show the results of an initial attempt to perform a "total-profile analysis" of the linter-guncotton. The reflections included in the refinement were the eight strongest cellulose trinitrate I reflections tabulated in reference 33. A crude amorphous profile was approximated as the smooth contour underlying the distinct meridional peaks in figure 1 of reference 32. A Compton contribution was determined as in the cellulose case. The least-square fit results are summarized in table 7.

The result of the total-profile analysis, although preliminary, represents the first such attempt for NC. In contrast, a large body of effort has been devoted in previous work to the characterization of the (101) reflection of NC for different degrees of nitration. Despite the effort, it is clear from figure 10 that even this aspect of NC structural characterization is not settled. We have determined the FWHM and d-spacing for the (101) reflection of each of our NC samples. To do this, the following simplifications were made:

1. We include both the (030) and (101) explicitly in the $9^\circ < \theta < 16^\circ$ refinement region, but fix the FWHM and θ_0 of (030) to be 1.5° and 10.3° respectively.
2. We assume the peak shapes of both reflections to be 50% Cauchy and 50% Gaussian.
3. We represent the "background" underneath the reflections by $A + B\theta + C^2$ and refine A, B, and C.

The results are summarized in table 8.

Nitrocellulose: Other Characterization

Mundy and co-workers (ref 4) have made an extensive study of the properties of NC prepared from the cellulose samples examined by us. They also studied properties of NC produced by current manufacturing processes. In this subsection we extract some of the results of Mundy et al. as they pertain to our samples.

In table 9 some of the properties of the woodpulp along with NC viscosity are listed. In figure 11 are shown the NC viscosity for pyrocotton and guncotton from the same cellulose feedstock grouped according to feedstock type. In figure 12 are shown solubility at 18% NaOH concentration of various pulps and Mullen Burst Strength versus crystallite dimension.

Studies by Mundy et al. of the rate of absorption of nitrating acids by the woodpulp indicate that the sulfate-processed pulps absorb at a higher rate than the sulfite pulps. Additionally, with P-1 acid (38.41% H_2SO_4 , 56.14% HNO_3 , 7.01% H_2O) the N-5 sulfate pulp absorbs at an anomalously high rate even in comparison with the other sulfate-processed pulps tested (not all were tested). Another property of interest confirmed by Mundy et al. was that the viscosity of high grade, baled-linter NC decreased with storage time compared to an increase of viscosity for sheeted pulp NC. They suggest that this is related to increased crystalline structure of NC fibers.

DISCUSSION

Cellulose

In the present work we have developed a comprehensive approach to the characterization of cellulose crystallographic properties using a total-profile analysis technique. In contrast to other studies of cellulose employing this approach, ours is the first which yields both lattice parameters and relative intensities in good agreement with the results of precise fiber measurements. The presence of texture in the samples was an aid in the analysis. In addition our results indicate that an explicit amorphous profile occurs in the diffraction patterns of celluloses (as proposed by Mann in ref 12, and others), and that a pure Cauchy line-shape for the Bragg peaks is probably not correct. Those methods which compare measured intensities at selected points to obtain an index of crystallinity we find to be of questionable value. Comparison of figures 3A and 5A, B, C, and D shows that in the $\theta = 18^\circ$ region the amorphous + Compton profile can be well below the total scattering profile and is quite sensitive to Bragg peak width.

Quantitatively, our range of values for percent-crystallinity (table 6) is consistent with some early work (see comparison in ref 37). In contrast our values (15 to 51%) are vastly different than the other total-profile analysis approaches (refs 17, 19, and 20) in which percent-crystallinities of 60 to 100% are obtained. As described earlier, however, the other total-profile approaches yield somewhat unsatisfactory lattice parameters and quite unsatisfactory relative intensities so that their percent-crystallinities should be considered with caution.

The Ruland approach, applied to celluloses in reference 16, yields percent-crystallinities in the range 35.6 to 56.2% - very much in agreement with our values. However, they find little difference between untreated and mercerized cottons of the same types. Although we have not performed the analogous measurements, our percent-crystallinity for Fortisan (cellulose II) is anomalously low and somewhat suspicious. It should be noted also that whereas our ball-milled cellulose is assumed to be 100% amorphous (as is commonly done) Viswanathan and Venkatakrishnan find it to be 28% crystalline. If we assume that 28% of our amorphous fractions are crystalline, we obtain values in the range 39 to 65% crystallinity.

From the point of view of our principal concern which is to identify critical cellulose parameters for NC production, table 6 shows the following:

1. Linter, sulfite, and sulfate pulps are differentiated fairly well by means of crystallite dimensions (i.e., L(002) and L(a)).
2. Crystallinity of linters is clearly greater than that of the woodpulp, but sulfite and sulfate pulps are not distinguishable on the basis of percent-crystallinity.
3. For the samples studied, sulfate pulps show greater sample-to-sample variability in all parameters than either sulfite pulps or linters.

Cellulose/Nitrocellulose Correlations

In this subsection we will indicate correlations in two different areas: the relationship of structural properties of cellulose with other properties and the correlation of structure and other cellulose properties with NC properties.

With reference to table 6 in which is summarized degree-of-crystallinity and crystallite size results, certain points should be noted. As mentioned previously, the linter samples are clearly different from the pulp samples both with regard to percent-crystallinity and crystallite size. Among the linter samples, measured parameters are remarkably similar except for one. The percent-crystallinity of sample 3 (sheet linter) is significantly less than that of the two baled linters.

The sulfite-process woodpulp samples are quite similar in both percent-crystallinity and crystallite size, whereas the sulfate-process samples show a wide range of values which includes those for the sulfite samples. As might be expected, cellulose solubility at 18% NaOH concentration shows an excellent correlation with crystallite size in the [002] direction (fig. 12a). All other factors being equal, the surface area exposed to solvent should be important in determining solubility. It is interesting to note that if a linear L(002) versus percent-solubility relation is assumed, both sample 6 and sample 11 exhibit anomalous behavior.

With regard to mechanical properties of cellulose, figure 12b shows several interesting features. As discussed in a previous subsection, Atalla (ref 21) has found that tensile strength and burst properties of paper increase with decreasing "crystallinity," actually FWHM(002); in our table 6, L(002) is inversely proportional to FWHM(002). In figure 12b, L(002) is plotted versus Mullen Burst Strength. The results are in excellent agreement with Atalla's observation with two notable exceptions: 1) the sulfite pulps exhibit a different strength/L(002) correlation than the sulfate pulps; and 2) sample 10 (Buckeye N-5) appears anomalous with respect to the other sulfate pulps. The fact that sulfite pulps differ from sulfate pulps in many respects has already been noted both in this work and by Mundy et al. (ref 4). Sample 10 exhibits apparently anomalous burst strength and also an anomalously high rate of absorption of P-1 nitrating acid. In our work, we have found that sample 10 is the only sample which contains a measurable amount of the cellulose II structure. Also, if a linear L(002) versus Mullen Burst Strength is assumed, sample 11 (Buckeye E-1) again exhibits anomalous behavior.

With regard to cellulose/NC correlations we have already noted that crystallite size and/or percent-crystallinity of the cellulose feedstock is "retained" in the NC (fig. 8). As Mundy et al. found for the cellulose properties they measured, we find no correlation between cellulose structural properties and degree of nitration in the NC derived therefrom.

In figure 11 we have replotted the NC viscosity data of Mundy et al. in groups according to the type of cellulose feedstock. Furthermore, we plot NC viscosity for pyrocotton and guncotton from the same feedstock to elucidate the possible differences in chemical heterogeneity of the various cellulose/NC samples. For each type of feedstock, but most clearly for the woodpulp, a correlation between cellulose viscosity and NC viscosity is apparent. More interesting is the sample-to-sample variation of the change in NC viscosity in going from pyrocotton to guncotton. For

example, compared to samples 1 and 2, sample 3 (sheet linters) shows an anomalously large increase in viscosity with increased percent nitrogen. Sample 3 also showed lower percent-crystallinity than samples 1 and 2. In the sulfite-pulp group, sample 6 also shows a relatively large change in viscosity with percent nitration. It also appeared to be somewhat anomalous in crystallite size/percent-solubility (fig. 12a), and, as mentioned previously, showed some "excess" scattering in the x-ray diffraction amorphous region which was not well-fit with our model.

The sulfate-pulp NC shows a variability comparable with that exhibited by the measured pulp structure parameters. If we assume that linter samples 1 and 2 represent "normal" changes in viscosity with percent nitrogen, all of the sulfate pulps, except sample 9, are abnormal. However, if we assume, based on all of the linter-NC and sulfite-pulp NC viscosities, that increasing nitration should produce significantly increased viscosities, then samples 10, 11, and to a lesser degree 12, appear abnormal. Sample 11, which exhibits a decrease in viscosity with increasing nitration, also is anomalous in percent-solubility and burst strength versus L(002) as shown in figure 12; sample 10 is anomalous in burst strength versus L(002). Sample 12, on the other hand, seems to exhibit regular behavior with respect to percent-solubility and burst strength.

In table 9 is listed the weight fractions of glucose, xylose, and mannose in the pulp samples. For the samples studied, only sample 11 has a composition which differs dramatically from the others. This compositional difference appears to manifest itself in all cellulose and NC properties that we have considered in this subsection except in degree of nitration. In contrast sample 10, which is the only sample in which cellulose II was detected, exhibits no compositional anomaly, but does exhibit a very high rate of absorption in addition to what has been noted above.

CONCLUSIONS

1. The total-profile technique of analyzing cellulose x-ray diffraction measurements, when properly formulated, yields:

- a. Relative peak intensities and lattice parameters consistent with fiber results.
- b. Best results when an explicit amorphous component is included.
- c. Amorphous-component fractions in fair, but not completely satisfactory, agreement with Kuland's method for similar samples.

2. The total-profile analysis of cellulose x-ray diffraction measurements for linter, sulfate- and sulfite-processed pulps suggests that criteria for acceptance of NC feedstocks should be established for each of the three types, separately.

3. The breadth of diffraction peaks, which depends on crystallite size, residual stress/strains, and defects, shows a correlation with both chemical and physical properties of cellulose.

4. The presence of even a small amount of cellulose II appears to affect both cellulose and NC properties significantly.

5. Both the crystallographic and nitration characteristics of NC (as manifested by viscosity) correlate with crystallographic properties of the cellulose feedstock.

RECOMMENDATIONS

1. The still-unresolved differences between the total-profile and Ruland methods of cellulose diffraction data analysis should be reconciled and understood.

2. The differences in crystallographic properties of NC from different feedstocks should be clarified, either by fiber studies and/or with hot-water treated NC in pellet samples.

3. The fact that viscosity of linter NC decreased with storage time while that of pulp NC increases has been attributed to different changes in "crystalline structure" (ref 4). This should be examined in a systematic way, both for the NC and the cellulose feedstock.

4. The correlation between mechanical properties and crystallinity and/or crystallite size, strains, and defects should be clarified and extended to NC.

5. The different viscosity characteristics of NC from sheet and baled linters should be examined relative to cellulose crystallinity of the feedstock for more samples.

REFERENCES

1. M. A. Millet, J. F. Saeman, and F. J. Masuelli, "Studies on the Characterization of Nitrating Pulps and Cellulose Nitrate--Final Report," Forest Products Laboratory, Madison, Wisconsin, November 24, 1958.
2. A. J. Bracuti, "The Determination of Cellulose Crystallinity," Technical Report ARLCD-TR-77078, ARRADCOM, Dover, NJ, August 1978.
3. H. J. Prask, C. S. Choi, R. Strecker, and E. Turngren, "Woodpulp Crystal Structure and Its Effect on Nitrocellulose Physical Properties," Technical Report ARLCD-TR-79031, ARRADCOM, Dover, NJ, September 1980.
4. R. A. Mundy, G. W. Elliott, J. A. Morris, R. A. Strecker, E. V. Turngren, and J. W. Leach, "Improved Nitrocellulose Process Controls," ARRADCOM Contractor Report ARLCD-CR-80029, Hercules Inc., Kenil, NJ, Radford AAP, Radford, VA, December 1980.
5. D. W. Jones, O. Ellefsen, and B. A. Tonnesen, "X-ray and Electron Diffraction," in High Polymers: Cellulose and Cellulose Derivatives (ed. N. M. Bikales and L. Segal) Part IV, vol V, 1971, Wiley Interscience, NY, pp 151-180.
6. Anatole Sarko, "What is the Crystalline Structure of Cellulose?" Tappi, vol 61, no. 2, 1978, pp 59-61.
7. H. J. Wellard, "Variation in the Lattice Spacing of Cellulose," Journal of Polymer Science, vol XIII, 1954, pp 471-476.
8. Francis J. Kolpak, Mark Weih, and John Blackwell, "Mercerization of Cellulose: I. Determination of the Structure of Mercerized Cotton," Polymer, vol 19, 1978, pp 123-131.
9. Carrie Woodcock and Anatole Sarko, "Packing Analysis of Carbohydrates and Polysaccharides. 11. Molecular and Crystal Structures of Native Ramie Cellulose," Macromolecules, vol 13, no. 5, 1980, pp 1184-1187.
10. J. A. Howsmon and W. A. Sisson, "Submicroscopic Structure," in High Polymers: Cellulose (ed. E. Ott and H. M. Spurlin) Part I, vol V, 1954, Interscience, NY, p 277.
11. R. Hosemann, "Crystallinity in High Polymers, Especially Fibres," Polymer, vol 3, 1962, pp 349-392.
12. J. Mann, "Modern Methods of Determining Crystallinity in Cellulose," Pure Appl. Chem. 5, 1962, pp 91-105.
13. V. W. Tripp, "Measurement of Crystallinity," in High Polymers: Cellulose and Cellulose Derivatives (ed. N. M. Bikales and L. Segal) Part IV, vol V, 1971, Wiley Interscience, NY, pp 305-323.
14. L. E. Alexander, "Degree of Crystallinity," X-ray Diffraction Methods in Polymer Science, 1969, Wiley Interscience, NY, pp 137-198.

15. W. Ruland, "X-ray Determination of Crystallinity and Diffuse Disorder Scattering," Acta Cryst. 14, 1961, pp 1180-1185.
16. A. Viswanathan and V. Venkatakrisnan, "Disorder in Cellulosic Fibers," Journal of Applied Polymer Science, vol 13, 1969, pp 785-795.
17. Jon Gjønnes, Nicolai Norman, and Henry Viervoll, "The State of Order in Cellulose as Revealed from X-ray Diffractograms," Acta Chemica Scandinavica 12, 1958, pp 489-494.
18. P. H. Hermans and A. Weidinger, "Quantitative Evaluation of the X-ray Diffraction of Ramie Fiber," Textile Research Journal 31, June 1961, pp 571-572.
19. A. M. Hindleleh and D. J. Johnson, "Crystallinity and Crystallite Size Measurement in Cellulose Fibres: 1. Ramie and Fortisan," Polymer, vol 13, September 1972, pp 423-430.
20. Hans Krassig, "Structure Investigations on Cellulose Fibers Using Infrared Spectroscopy and X-ray Diffraction," Applied Polymer Symposium, no. 28, 1976, pp 777-790.
21. Rajai H. Atalla, "The Crystallinity of Cellulosic Fibers," Adv. Chem. Ser. 193, 1981, pp 169-176.
22. Kh. M. Mannan and M. Reazuddin, "Crystallinity for Natural Cellulose in Jute Fibre," Indian J. Phys. 52A, 1978, pp 130-136.
23. "Absorption," International Tables for X-ray Crystallography, vol III, 1968, pp 157-199.
24. D. T. Keating and G. H. Vineyard, "The Complete Incoherent Scattering Function for Carbon," Acta Cryst. 9, 1956, pp 895-896.
25. R. McWeeny, "X-ray Scattering by Aggregates of Bonded Atoms. I. Analytical Approximations in Single-Atom Scattering," Acta Cryst. 4, 1951, pp 513-519.
26. A. J. Freeman, "X-ray Incoherent Scattering Functions for Non-Spherical Charge Distributions: N, N⁻, O⁻, O, O⁺, O⁺², O⁺³, F, F⁻, Si⁺⁴, Si⁺³, Si, and Ge," Acta Cryst. 12, 1959, pp 929-936.
27. L. Segal, J. J. Creely, A. E. Martin, Jr., and C. M. Conrad, "An Empirical Method for Estimating the Degree of Crystallinity of Native Cellulose Using the X-ray Diffractometer," Textile Research Journal 29, 1959, pp 786-794.
28. M. A. Ivanov and A. L. Kosoy, "Rapid X-ray Diffraction Technique for Determination of Crystallinity of Cellulosic Materials," Journal of Applied Polymer Science, vol 19, 1975, pp 2353-2357.
29. J. Mann, L. Roldan-Gonzalez, and H. J. Wellard, "Crystalline Modifications of Cellulose. Part IV. Determination of X-ray Intensity Data," Journal of Polymer Science, vol XLII, 1960, pp 165-171.

30. Anatole Sarko and Reto Muggli, "Packing Analysis of Carbohydrates and Polysaccharides. III. Valonia Cellulose and Cellulose II," Macromolecules, 7, 1974, pp 486-494.
31. T. Urbanski, "Cellulose and Nitrocellulose," in Chemistry and Technology of Explosives, vol II, ch. IX, Pergammon Press, London, 1965, pp 213-292.
32. Sadayoshi Watanabe, Jisuke Hayashi, and Kiyoshiimai, "A Study of Cellulose Trinitrate Structure," Journal of Polymer Science, Part C, no. 23, 1968, pp 809-823.
33. S. Watanabe, K. Imai, and J. Hayashi, "On the Existence of Cellulose Trinitrate II," Chemical Society of Japan: Journal (Industrial Chemistry Section), 74, 1971, pp 1420-1426.
34. S. Watanabe, K. Imai, and J. Hayashi, "Crystal Structures of Cellulose-Trinitrates Derived from Various Crystalline Modifications of Cellulose," Chemical Society of Japan: Journal (Industrial Chemistry Section), 74, 1971, pp 1427-1431.
35. J. Hayashi, K. Imai, T. Hamazaki, and S. Watanabe, "On the Existence of Cellulose Dinitrate Crystallite," Japanese Journal of Chemistry, no. 8, 1973, pp 1582-1587.
36. J. Hayashi, K. Imai, T. Hamazaki, and S. Watanabe, "Crystalline Structures of Cellulose Dinitrates and Their Saponification Products Derived from Various Crystalline Modifications of Cellulose," Japanese Journal of Chemistry, no. 8, 1973, pp 1587-1591.
37. R. Bonart, R. Hosemann, F. Motzkus, and H. Ruck, "X-ray Determination of Crystallinity in High-Polymeric Substances," Norelco Reports, 7, 1960, pp 81-97.

Table 1. Cellulose samples

<u>Sample</u>	<u>Source</u> ^a	<u>Type</u>
1	Buckeye	linter (baled)
2	Hercules	linter (baled)
3	Hercules NS 70	linter (sheet)
4	Fortisan	
5	Alaska	sulfite pulp
6	Ga. Pacific Puget 92	sulfite pulp
7	I.P.C. BH-C	sulfate pulp
8	I.P.C. Acetakraft	sulfate pulp
9	Buckeye N-7	sulfate pulp
10	Buckeye N-5	sulfate pulp
11	Buckeye E-1	sulfate pulp
12	Buckeye V-60	sulfate pulp

^a More complete details are given in reference 4.

Table 4. Fortisan: lattice parameters and peak intensities

	<u>This work</u>	<u>Mercerized cotton^b</u>	<u>Fortisan^c</u>	<u>Various samples^d</u>
A(Å)	8.045±0.003	8.02	7.92	7.83-8.04
B(Å)	(10.36) ^a	10.36	10.34	--
C(Å)	9.195±0.002	8.99	9.08	9.05-9.29
β(deg)	62.7±0.03	63.4	62.7	62.2-63.4
I(101)	0.141±0.004	0.129	0.111	--
I(10 $\bar{1}$)	0.90±0.03	0.89	1.00	--
I(002)	1.0	1.00	1.00	--

^a Fixed from ref 8.

^b Ref 8

^c Refs 12 and 29.

^d Ref 7, but excluding mercerized linen as somewhat atypical.

Table 5. Woodpulp: lattice parameters and peak intensities

Parameter	Sample	
	5	6
A(Å)	8.15±0.02	8.16±0.02
B(Å)	(10.34) ^a	(10.34)
C(Å)	7.911±0.001	7.905±0.001
B(deg)	84.04±0.03	83.97±0.03
I(101)	0.113±0.005	0.122±0.005
I(10 $\bar{1}$)	0.151±0.006	0.118±0.006
I(021)	0.011±0.001 ^b	0.022±0.001
I(002)	1.0	1.0
I(101)+10 $\bar{1}$)	0.264 ^c	0.240

^a Fixed from ref 9.

^b FWHM(021) fixed = FWHM(002); standard deviation from peak height only.

^c To be compared with 0.244 (= average linter value).

Table 5. (cont)

Parameter	Sample											
	7	8	9	10	11 ^d	12						
A(Å)	8.15±0.02	8.11±0.02	8.15±0.02	8.08±0.02	8.01±0.02	8.13±0.02						
B(Å) ^a	(10.34)	(10.34)	(10.34)	(10.34)	(10.34)	(10.34)						
C(Å)	7.894±0.001	7.891±0.001	7.892±0.001	7.901±0.001	7.949±0.001	7.917±0.001						
β(deg)	84.71±0.03	84.63±0.03	84.54±0.03	84.34±0.04	83.94±0.04	84.39±0.04						
I(101)	0.106±0.004	0.119±0.004	0.102±0.004	0.120±0.005	0.100±0.005	0.110±0.005						
I(101̄)	0.128±0.005	0.122±0.005	0.145±0.006	0.114±0.006	0.186±0.010	0.162±0.007						
I(021) ^b	0.015±0.001	0.017±0.001	0.021±0.001	0.022±0.002	0.030±0.001	0.008±0.001						
I(002)	1.0	1.0	1.0	1.0	1.0	1.0						
I(101+101̄) ^c	0.234	0.241	0.247	0.234	0.286	0.272						

^a Fixed from ref 9.

^b FWHM(021) fixed = FWHM(002); standard deviation from peak height only.

^c To be compared with 0.244 (= average Iinter value).

^d See discussion in text.

Table 6. Celluloses: crystallinity, particle sizes, and shape parameters

Sample	Type	% Crystallinity	f_{Cauchy}	$L(002)^a$ (Å)	$L(a)^b$ (Å)
1	I-linter	49.1 \pm 2.0	0.616 \pm 0.014	73.2 \pm 0.4	50.2 (+0.6) ^c
2	I-linter	50.8 \pm 1.5	0.613 \pm 0.010	75.5 \pm 0.3	50.6 (+0.7)
3	I-linter	44.1 \pm 1.6	0.596 \pm 0.010	75.8 \pm 0.3	50.6 (-0.7)
5	I-sulfite	35.1 \pm 2.2	0.545 \pm 0.014	47.2 \pm 0.2	36.3 (+0.2)
6	I-sulfite	36.0 \pm 1.7	0.549 \pm 0.015	47.9 \pm 0.2	36.1 (-3.2)
7	I-sulfate	32.4 \pm 2.0	0.660 \pm 0.013	55.8 \pm 0.3	41.9 (+0.5)
8	I-sulfate	35.4 \pm 1.9	0.685 \pm 0.012	57.5 \pm 0.3	41.6 (-1.7)
9	I-sulfate	37.2 \pm 2.0	0.585 \pm 0.012	52.1 \pm 0.2	40.0 (+1.5)
10	I-sulfate	32.3 \pm 2.1	0.838 \pm 0.015	56.5 \pm 0.3	40.1 (-3.7)
11	I-sulfate	43.2 \pm 2.3 ^d	(0.6) ^d	42.1 \pm 0.2	34.8 (+2.9)
12	I-sulfate	26.7 \pm 3.3	0.474 \pm 0.016	48.1 \pm 0.3	38.7 (+1.8)
4	II-Fortisan	15.4 \pm 2.2	0.526 \pm 0.012	61.6 \pm 0.6	45.4 (-6.5)

^a From Debye-Scherrer eqn.: $L(hkl) = \lambda / (\text{FWHM} \cos(\theta/2))$.

^b From $L(101)$ and $L(10\bar{1})$ as shown in figure 7.

^c $L(a) - L(10\bar{1})$ = value in parenthesis.

^d See discussion in text.

Table 7. Total profile refinement parameters for 13.5 wt% N, linter NC

<u>Parameter</u>	<u>Value</u>	<u>Parameter</u>	<u>Value</u>
A(Å)	12.29±0.04	Ht(150)	28.0
B(Å)	(25.75) ^a	FWHM(150)	(2.0) ^c
C(Å)	8.93±0.01	Ht(161)	0. ^d
Ht(050) ^b	17.0	FWHM(161)	--
FWHM(050)	(1.5) ^c	Ht(070)	100.0
Ht(101)	39.8	FWHM(070)	(2.0) ^c
FWHM(101)	1.50	Ht(202)	0. ^d
Ht(012)	81.8	FWHM(202)	--
FWHM(012)	(2.0) ^c	Ht(170)	0. ^d
Ht(180)	0. ^d	FWHM(170)	--
FWHM(180)	--	AMOR. AMPL.	.23 ^e
Ht(0·10·0)	25.0	f _{cauchy}	.667 ^c
FWHM(0·10·0)	3.49		

^a Fixed from ref 33.

^b Ht = peak height.

^c Arbitrarily chosen.

^d Refined to ~ 0.

^e Refined but unnormalized.

Table 8. d-spacing and FWHM of NC(101) reflection

<u>Wt% N</u>	<u>Source</u>	<u>FWHM(deg)</u>	<u>d(Å)</u>
13.53	1-Linter	1.79 \pm 0.07	7.23 \pm 0.01
13.50	2-Linter	1.74 \pm 0.05	7.23 \pm 0.01
13.41	5-Sulfite	1.52 \pm 0.07	7.18 \pm 0.01
13.48	6-Sulfite	1.54 \pm 0.04	7.15 \pm 0.01
13.43	7-Sulfate	1.69 \pm 0.05	7.16 \pm 0.01
13.50	8-Sulfate	1.56 \pm 0.06	7.16 \pm 0.01
13.44	9-Sulfate	1.52 \pm 0.06	7.14 \pm 0.01
13.45	10-Sulfate	1.63 \pm 0.04	7.15 \pm 0.01
12.76	5-Sulfite	1.73 \pm 0.07	7.05 \pm 0.01

Table 9. Various other properties of celluloses

Sample	Cellulose ^a viscosity (sec)	Mullen ^b burst strength (lbs)	NC viscosity (sec) ^a		Fiber species	Glucose	Xylose (wt%)	Mannose
			13.4	12.6				
1-linter	12.9	c	206.8	166.5	cotton	c	c	c
2-linter	11.6	c	217.5	172.7	cotton	c	c	c
3-linter	13.4	c	259.2	178.3	cotton	c	c	c
5-sulfite	8.52	77	174.5	129.1	e	96.5	1.5	1.4
6-sulfite	17.65	64	308.1	185.8	e	94.7	1.9	2.9
7-sulfate	12.37	69	215.7	133.2	oak, gum	98.0	1.3	trace
8-sulfate	12.01	34	200.2	134.2	oak, gum	97.8	1.4	trace
9-sulfate	11.00	85	185.6	146.6	so. pine	95.6	2.2	1.7
10-sulfate	10.50	100	146.5	140.4	so. pine	98.2	0.6	0.8
11-sulfate	14.00	145	183.2	188.0	so. pine	84.8	7.6	7.0
12-sulfate	5.20	137	120.0	106.8	so. pine	95.8	2.1	1.6
13 ^d -sulfite	15.31	77	233.3	187.4	so. pine	93.5	2.8	3.1

^a From table 8, ref 4.

^b From table 10, ref 4 (for celluloses).

^c Not reported.

^d IIT Rayonier (sulfite); not studied with x-ray diffraction.

^e Mixed northwest spruce, pine, fir.

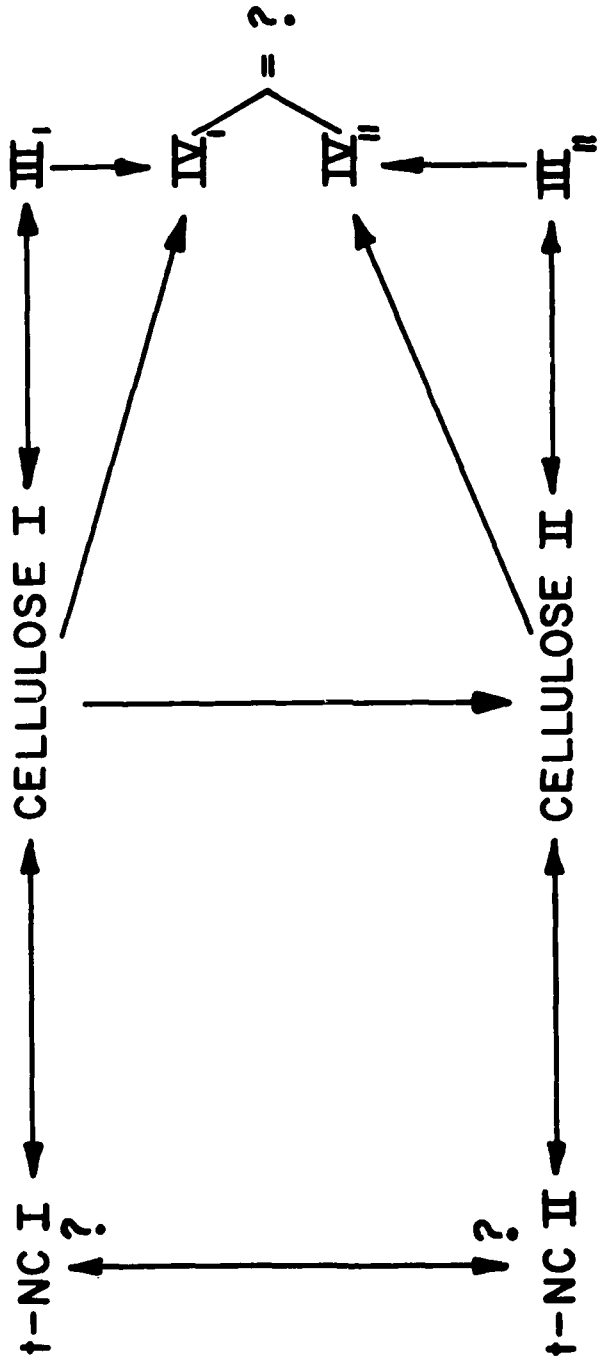
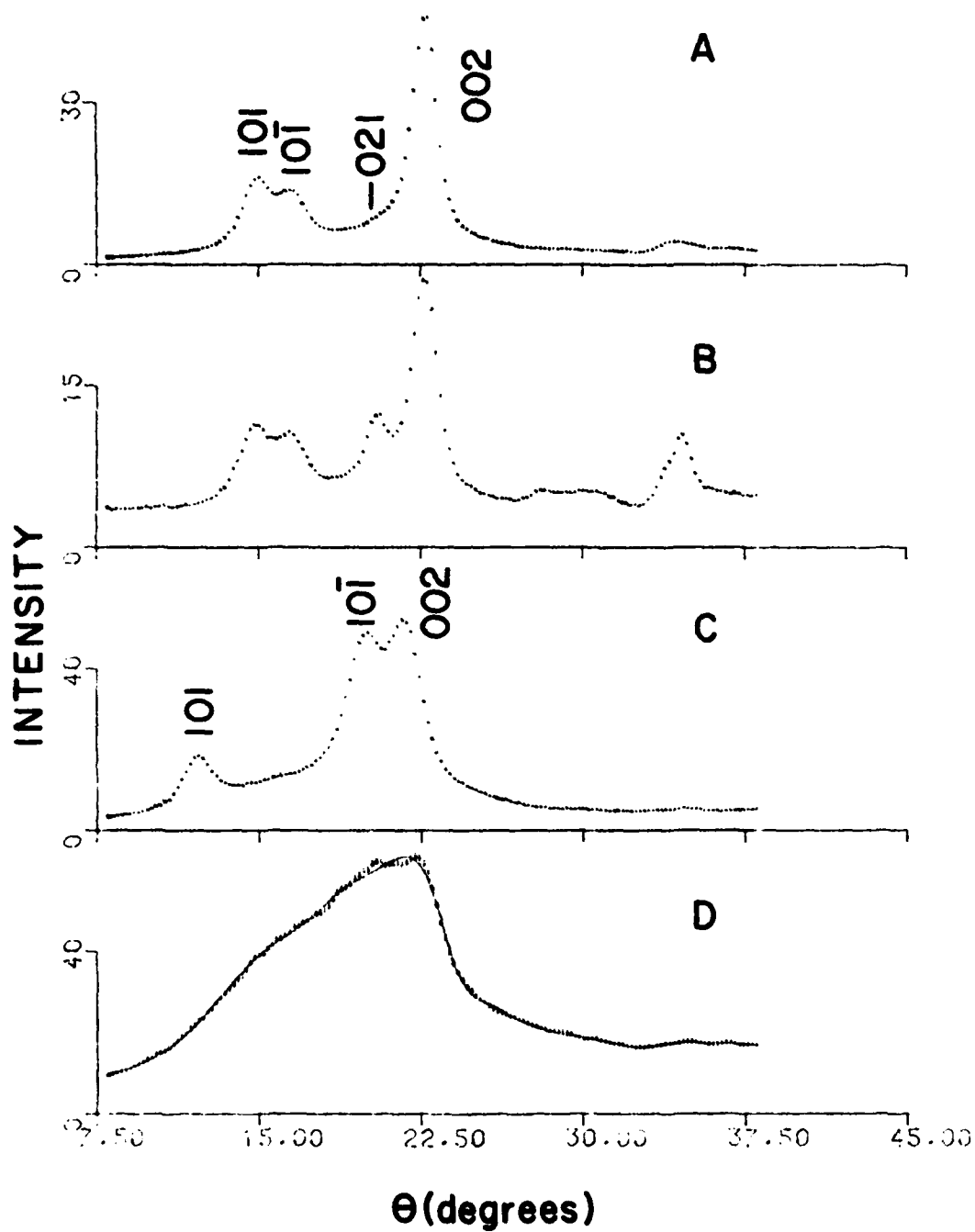
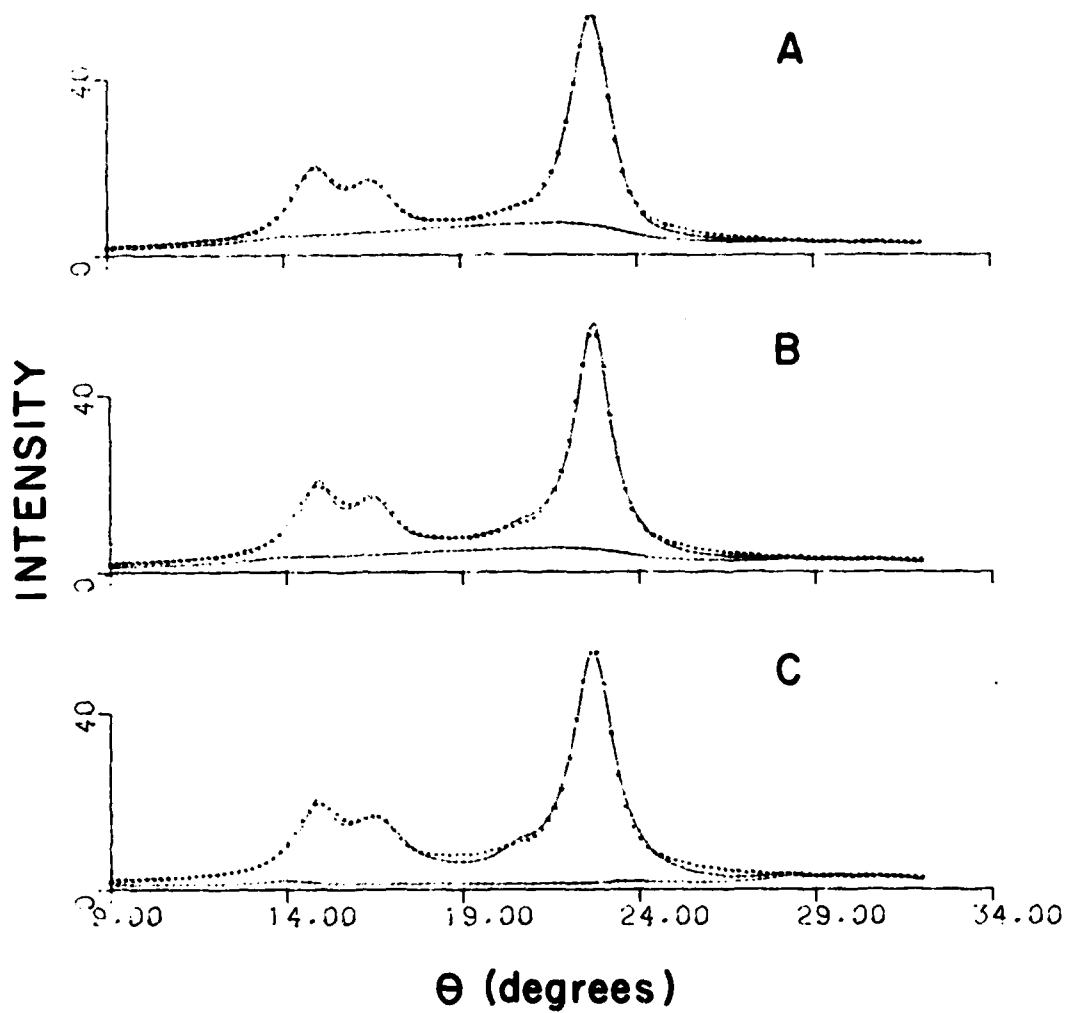


Figure 1. Crystallographic phases and possible interconversions of cellulose and tri-nitrocellulose polymorphs



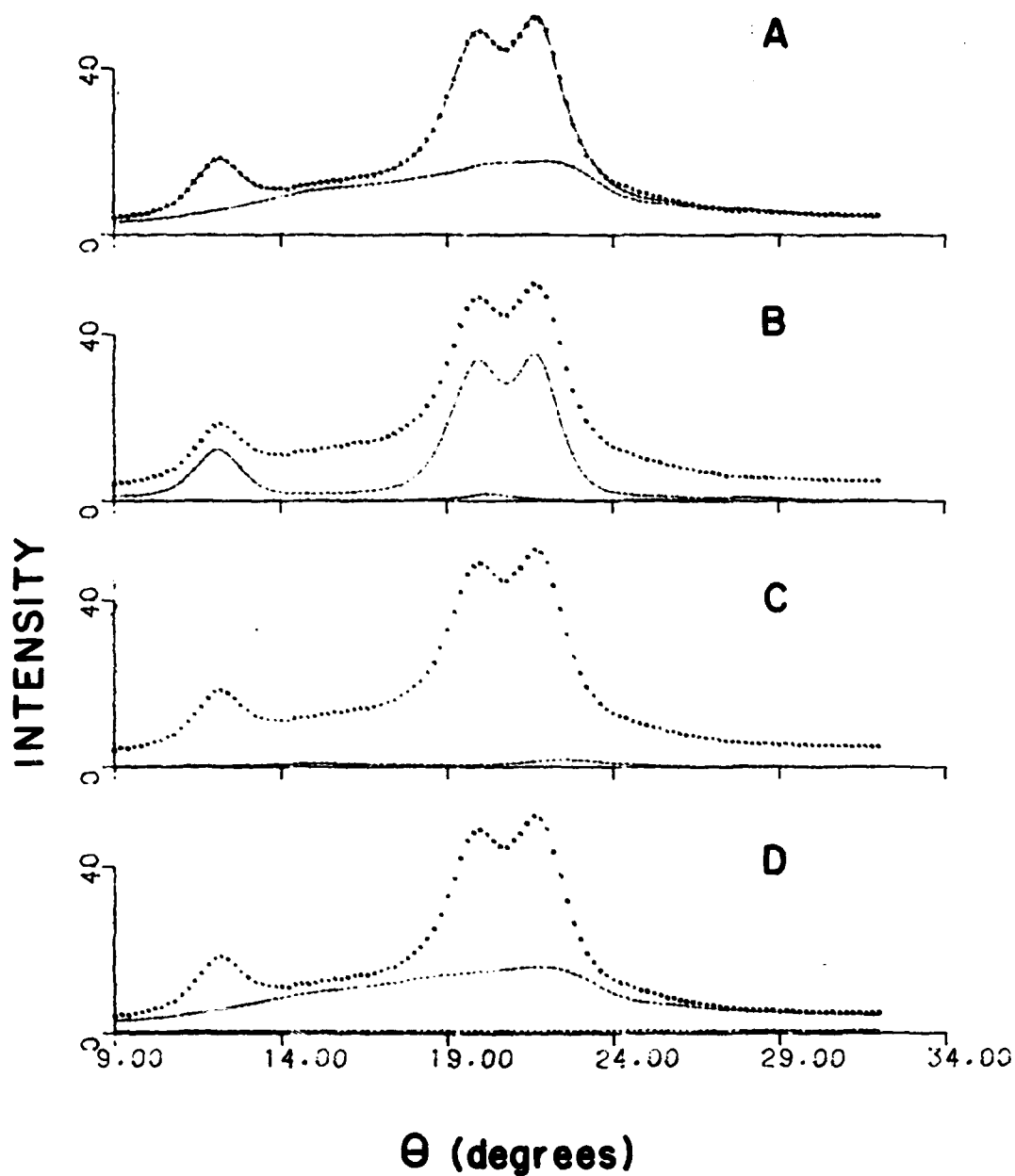
A = cellulose I (Hercules linters, reflection); B = cellulose I (Hercules linters, transmission); C = cellulose II (Fortisan, reflection); D = "amorphous" cellulose with analytical fit

Figure 2. X-ray diffraction patterns for various celluloses



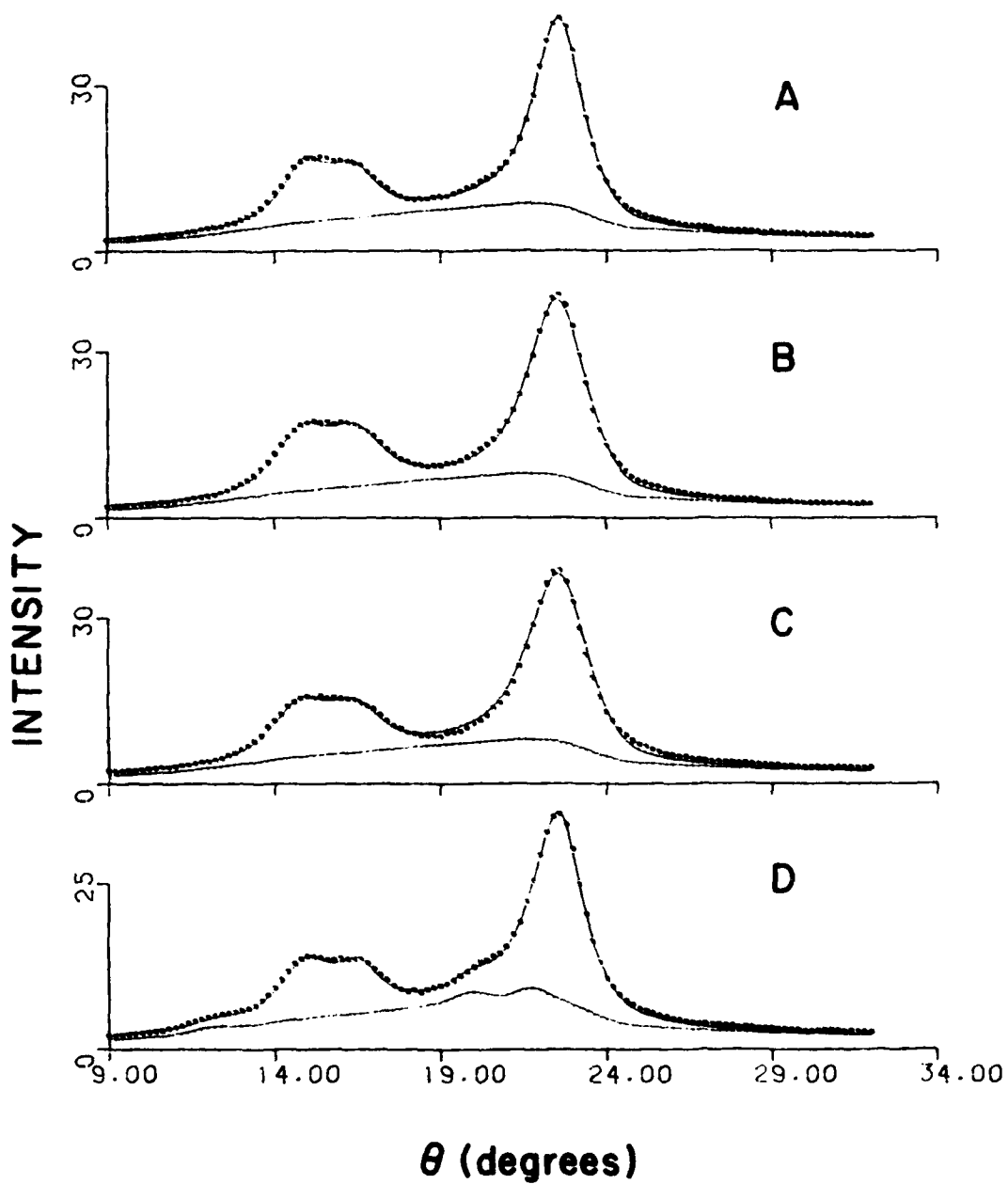
A = Cauchy/Gaussian fraction and amorphous amplitude varied;
 B = amorphous amplitude varied; C = no amorphous contribution

Figure 3. X-ray diffraction pattern of Hercules NS-70 (sheet) liners with total-profile fits and (amorphous + Compton + secondary Bragg peaks) contribution



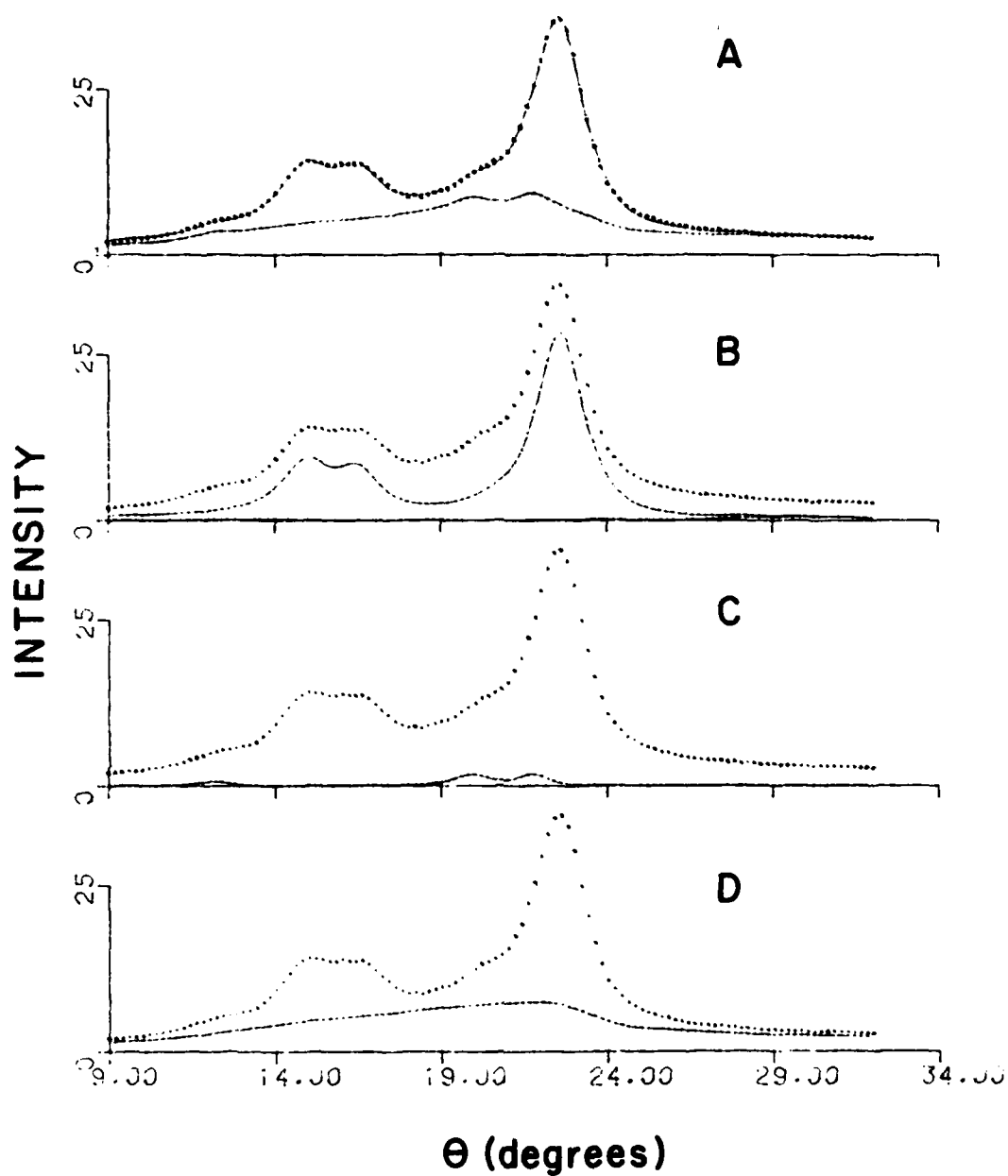
A = total profile fit and (amorphous + Compton + secondary Bragg peaks + cellulose I); B = [(101) + (101) + (002)] and secondary phase II peaks; C = cellulose I (1.9 wt% = 12.1% of crystalline fraction); D = amorphous and Compton

Figure 4. X-ray diffraction pattern of cellulose II with various calculated contributions



A = IPC BH-C sulfate (sample 7); B = Alaska sulfite (5);
 C = Ga. Pacifac Puget 92 sulfite (6); D = Buckeye N-5
 sulfate (10)

Figure 5. X-ray diffraction patterns of various woodpulp celluloses with total-profile fits and (amorphous + Compton + secondary Bragg peaks + cellulose I) contributions



A = total-profile fit and (amorphous + Compton + secondary Bragg peaks + cellulose II) contribution; B = cellulose I contribution; C = cellulose II contribution (~ 1 wt% = 2.6% of crystalline fraction); D = amorphous + Compton

Figure 6. X-ray diffraction pattern of Buckeye N-5 with various calculated contributions

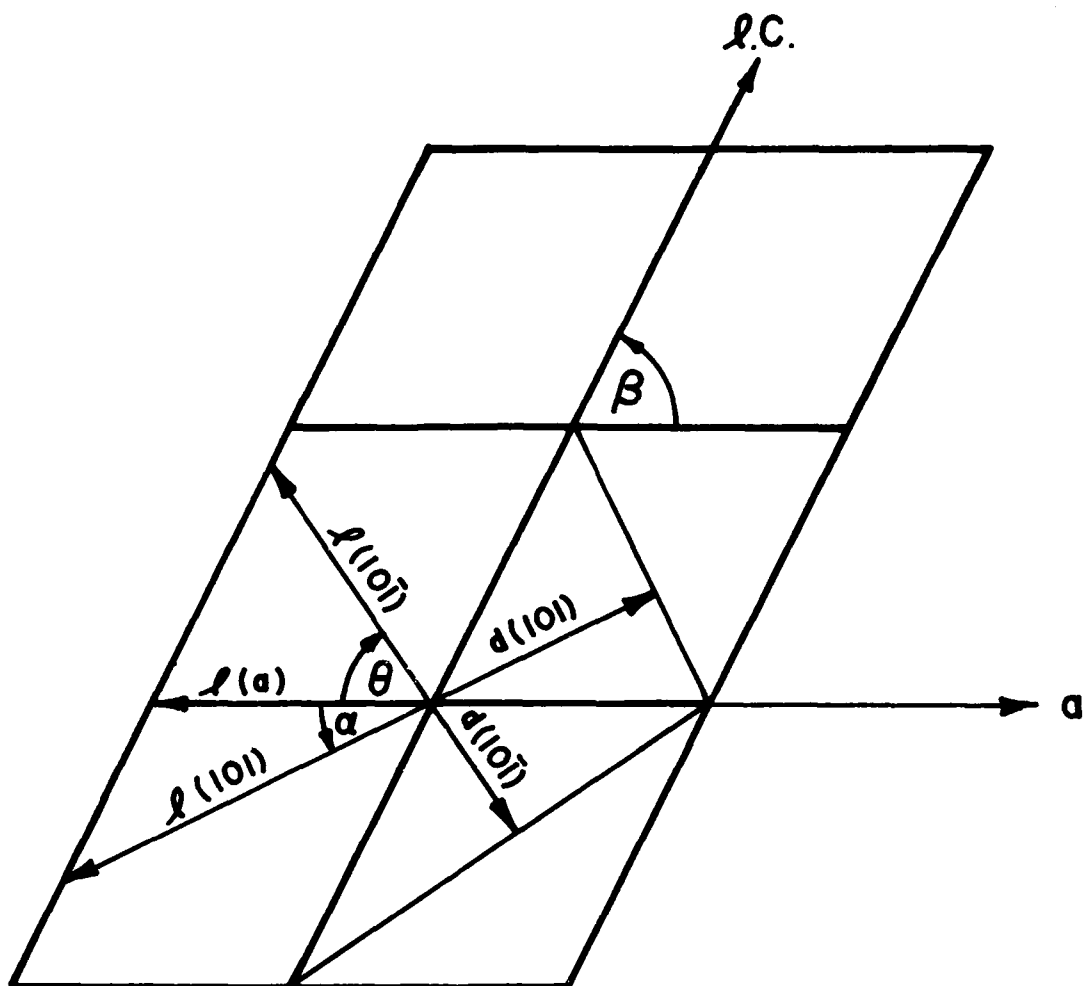
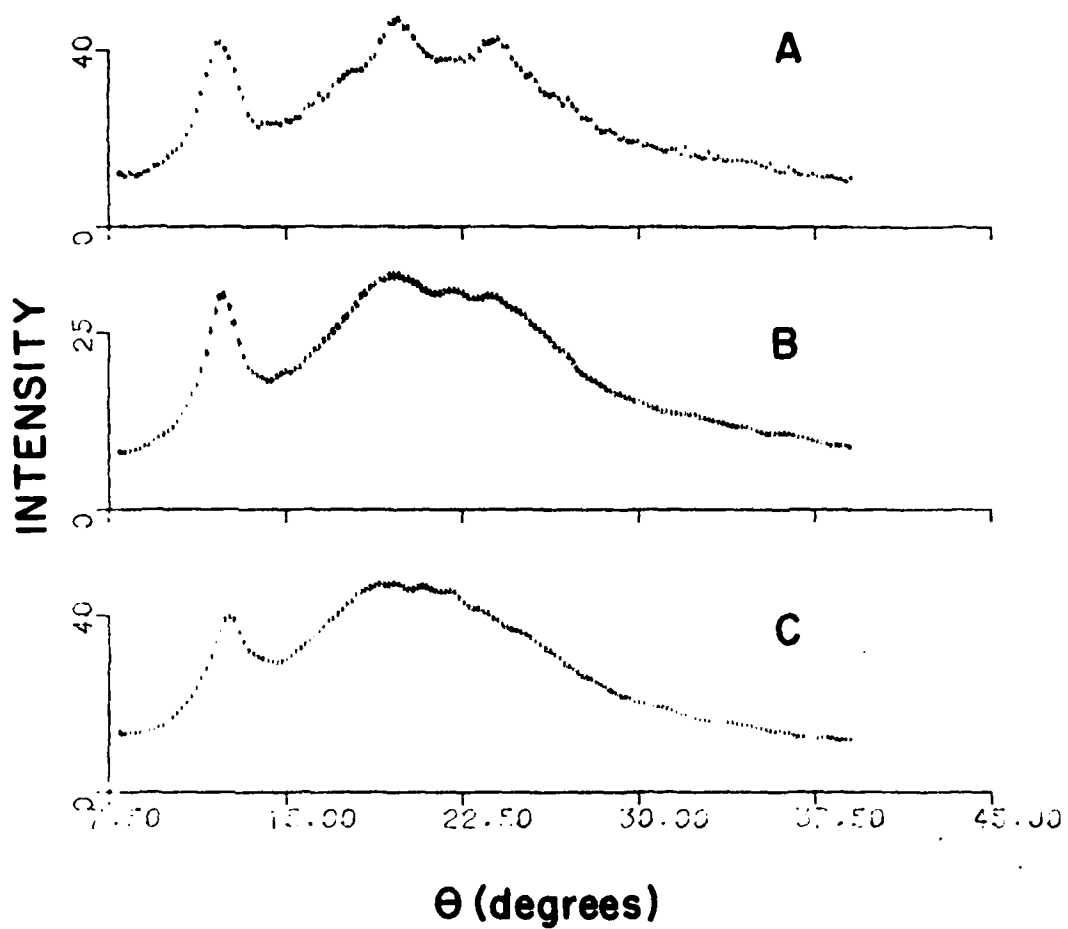


Figure 7. Schematic representation of unit cells comprising a cellulose I crystallite, viewed along the chain axis with crystallite dimensions for various directions indicated ($2l = L$ of table 6)



A = guncotton (13.5%N) from Hercules linters; B = guncotton (13.41%N) from Alaska sulfite pulp; C = pyrocotton (12.16%N) from Alaska sulfite pulp

Figure 8. X-ray diffraction patterns of selected NC samples

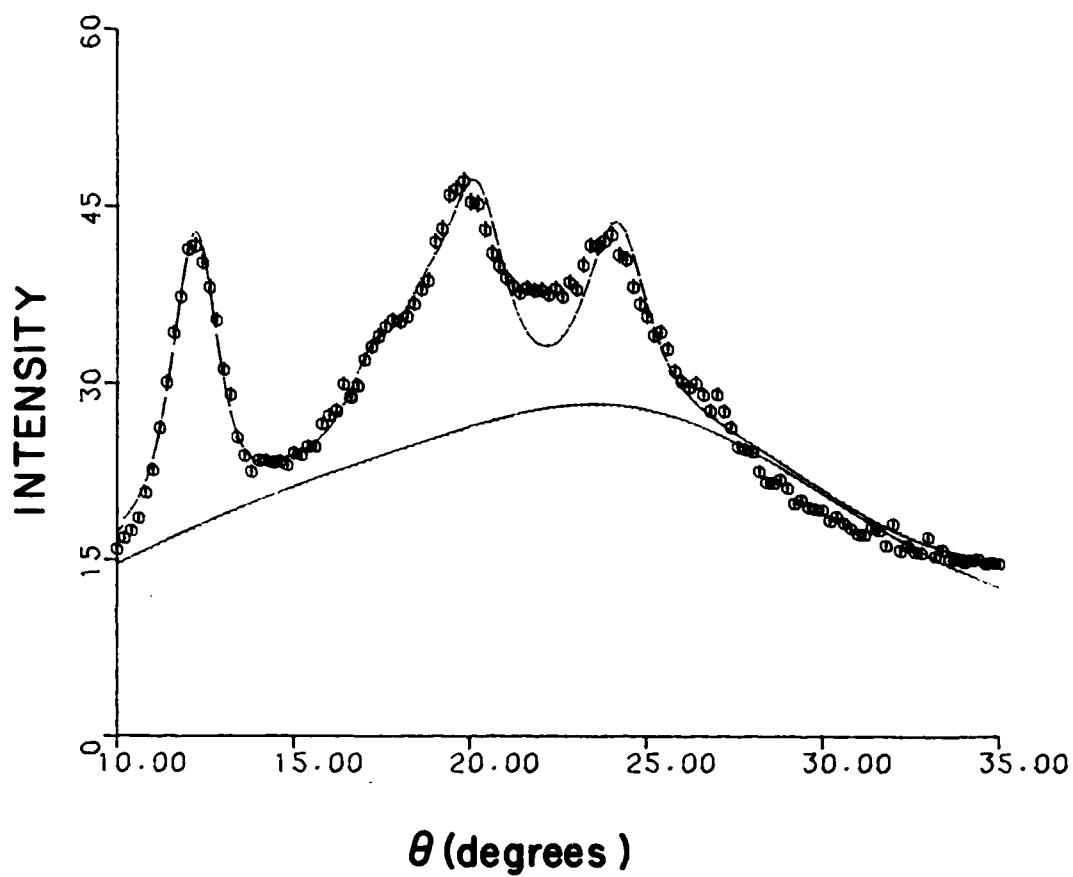
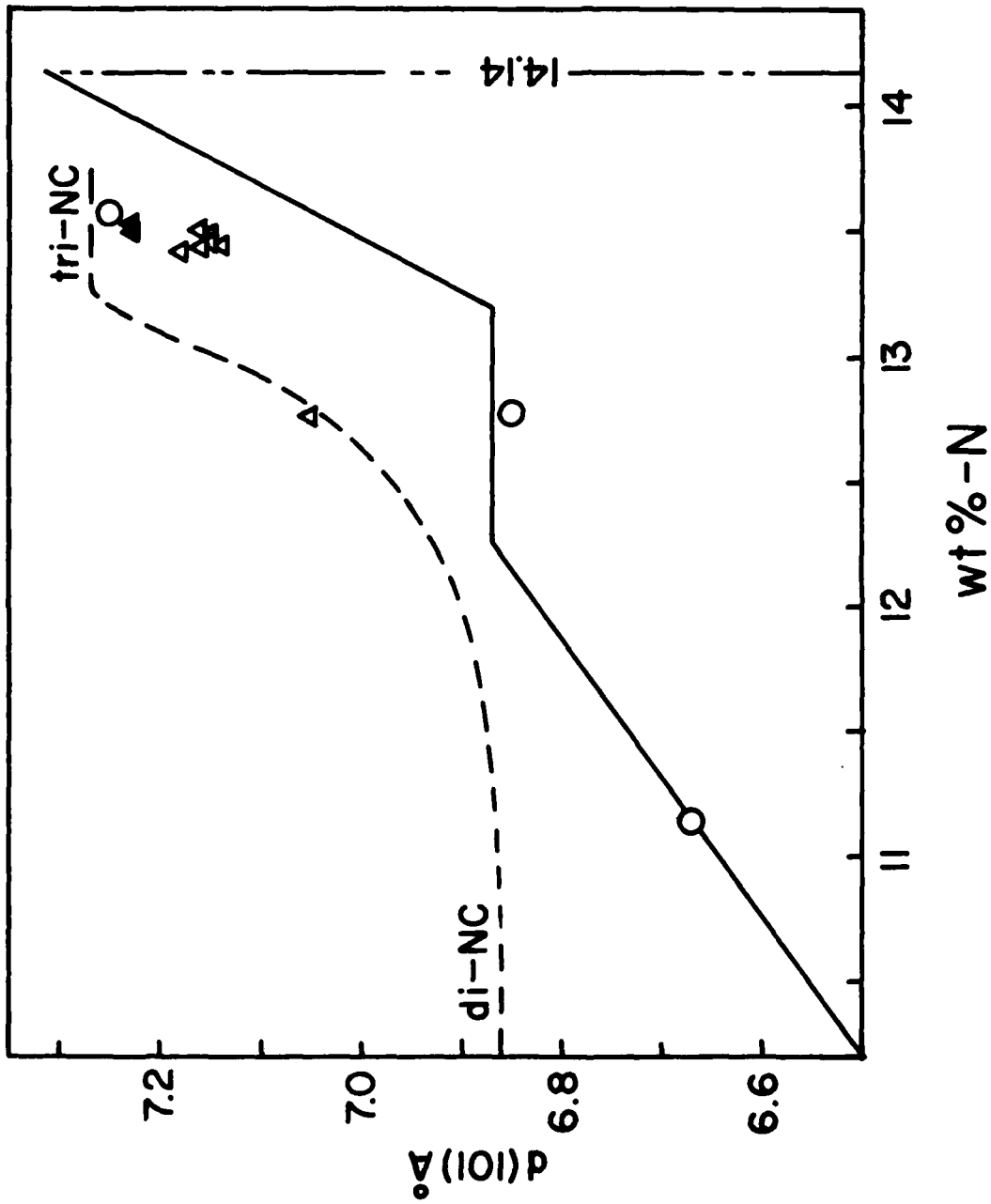


Figure 9. X-ray diffraction pattern of Hercules-linter guncotton with total-profile fit and amorphous contribution using parameters of table 7



open circles and curves from reference 31 (p. 239); closed triangles = linter NC, open triangles = pulp NC, both from present work

Figure 10. d(101) versus percent nitrogen

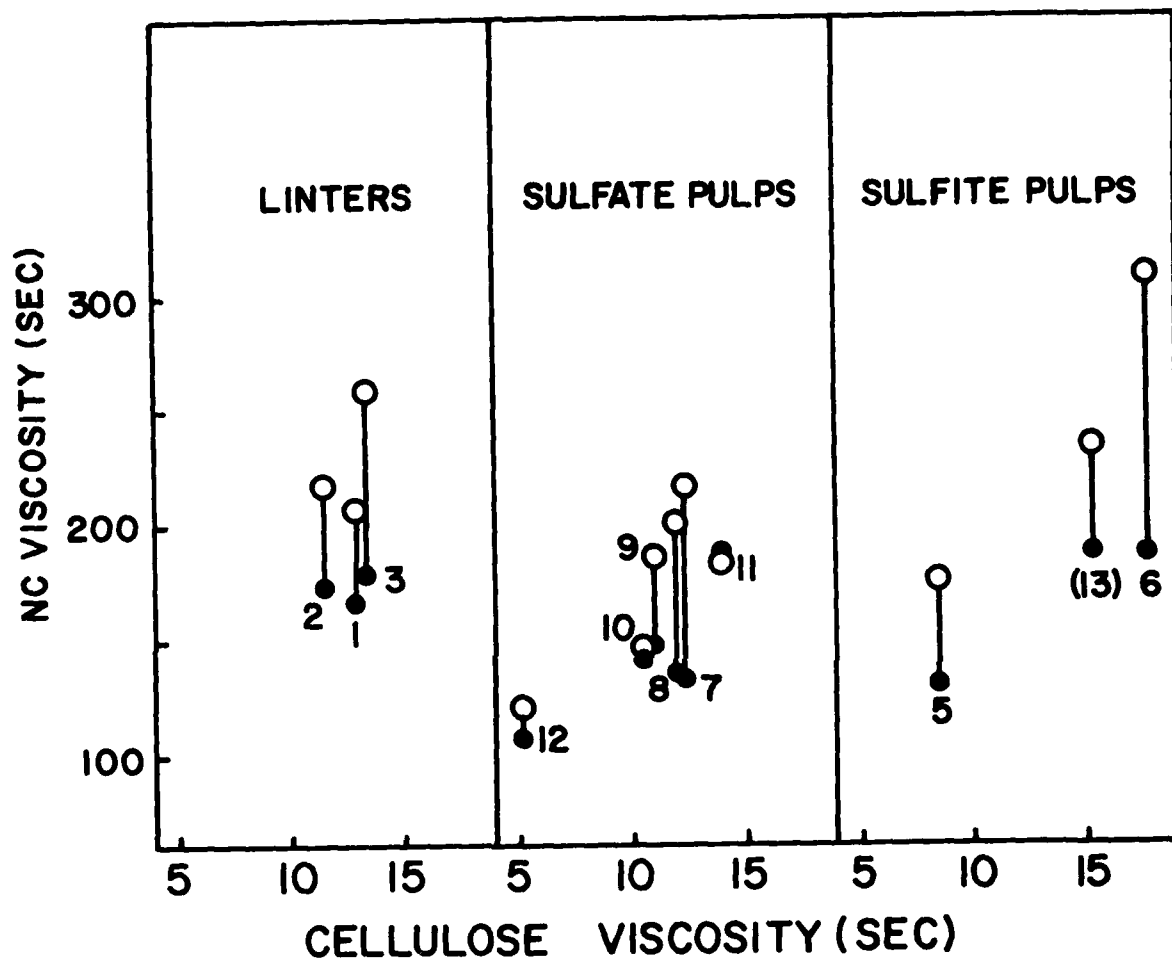
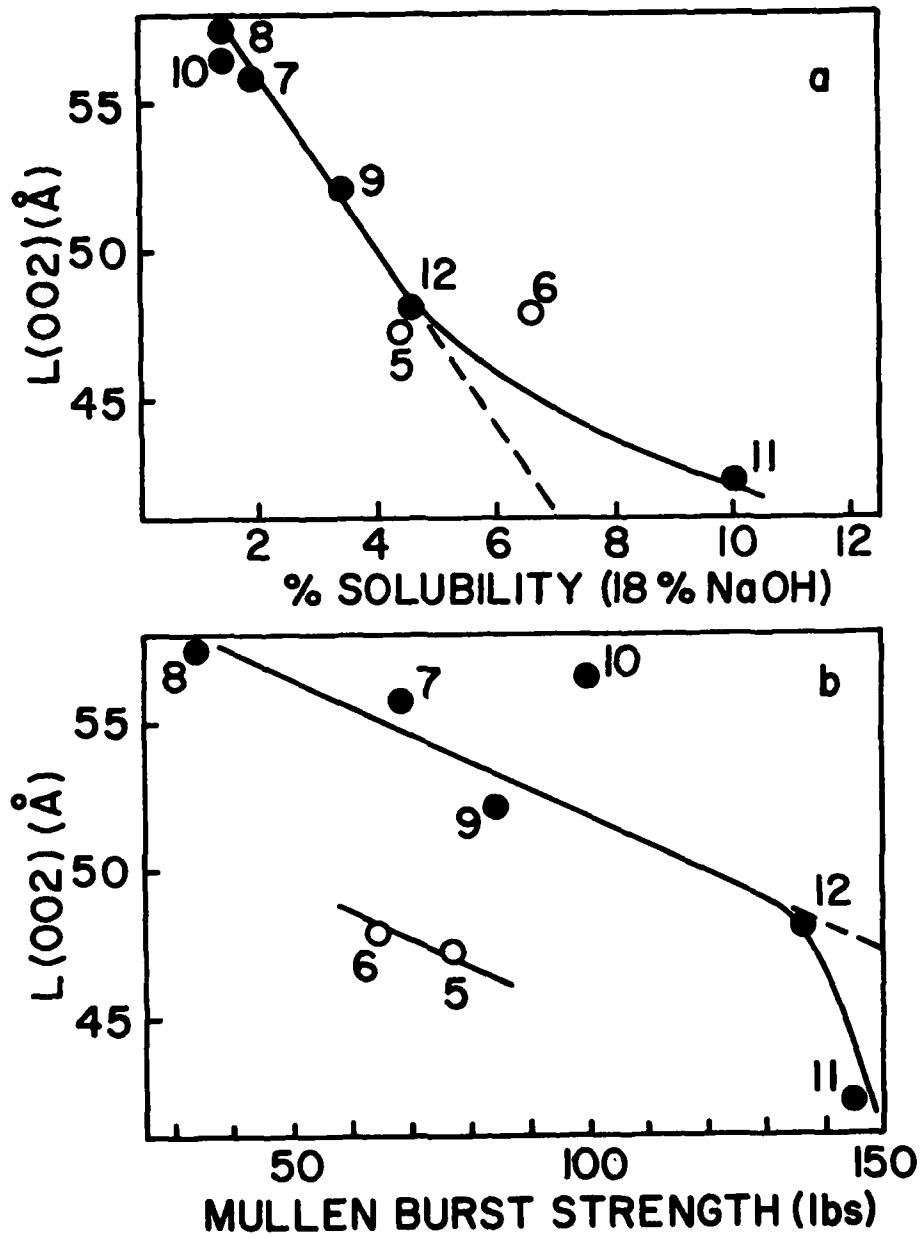


Figure 11. NC viscosity versus cellulose viscosity for pyrocottons (closed circles) and guncottons (open circles)



Closed circles = sulfate pulps, open circles = sulfite pulps

Figure 12. Crystallite (002) dimension versus percent-solubility and Mullen Burst Strength for woodpulp

DISTRIBUTION LIST

Commander
U.S. Army Materiel Development and
Readiness Command

ATTN: DRCDE
DRCMT
DRCPA
DRCPP-I
DRCPI
DRCSC

5001 Eisenhower Avenue
Alexandria, VA 22333

Commander
U.S. Army Armament Research and
Development Command

ATTN: DRDAR-CG
DRDAR-GCL
DRDAR-LCA, Dr. J. Lannon
Dr. Y. Carignon
Mr. A. Bracuti
Dr. A. Beardell
Dr. D. Downs
Mr. C. Lenchitz
Mr. S. Bernstein
Mr. E. Costa
Mr. A. Grabowsky
DRDAR-LCE, Dr. R. Walker (3)
Dr. J. Mikula
Dr. H. Prask (10)
Dr. C. Choi (10)
Dr. R. Strecker
Mr. E. Turngren
Dr. P. Marinkas
Dr. D. Wiegand

DRDAR-LCM
DRDAR-LCU
DRDAR-SCA, Dr. B. Brodman
DRDAR-SF
DRDAR-TSS (5)

Dover, NJ 07801

Commander
U.S. Army Munitions Production Base Modernization Agency
ATTN: SARPM-PBM-EP
Dover, NJ 07801

Commander
U.S. Army Armament Materiel
Readiness Command
ATTN: DRSAR-ASF
DRSAR-IR
DRSAR-IRC
DRSAR-IRM
DRSAR-LC
DRSAR-LEP-L
DRSAR-PDM
DRSAR-SF
Rock Island, IL 61299

Commander
Radford Army Ammunition Plant
ATTN: SARRA-EN (2)
Radford, VA 24141

Commander
U.S. Naval Ordnance Station
Indianhead, MD 20640

Commander/Director
Chemical Systems Laboratory
U.S. Army Armament Research and
Development Command
ATTN: DRDAR-CLB-PA
DRDAR-CL
DRDAR-CLJ-L
APG, Edgewood Area, MD 21010

Administrator
Defense Technical Information Center
ATTN: Accessions Division (12)
Cameron Station
Alexandria, VA 22314

Director
Ballistic Research Laboratory
U.S. Army Armament Research and
Development Command
ATTN: DRDAR-BLE (2)
DRDAR-TSB-S
Aberdeen Proving Ground, MD 21005

Chief
Benet Weapons Laboratory, LCWSL
U.S. Army Armament Research and
Development Command
ATTN: DRDAR-LCB-TL
Watervliet, NY 12189

Commander
U.S. Army Research Office
ATTN: Dr. D. Squire
Research Triangle Park, NC 27709

Commander
U.S. Army Foreign Science and
Technology Center
Charlottesville, VA 22902

Director
U.S. Army Materiel Systems Analysis Activity
ATTN: DRXSY-MP
Aberdeen Proving Ground, MD 21005

Director
U.S. Army TRADOC Systems
Analysis Activity
ATTN: ATAA-SL
White Sands Missile Range, NM 88002

ME
8